Metabolic Trans-Omic Analysis Reveals Key Regulatory Disruption of Energy Metabolism in Alzheimer's Disease

Tomoharu Katayama[1], Hikaru Sugimoto[2], Keigo Morita[2, 3], Hirohisa Watanabe[4], and Shinya Kuroda[2,3,5*]

Affiliations

[1]Department of Medicine, Faculty of Medicine, The University of Tokyo, 7-3-1 Hongo, Bunkyo-ku, Tokyo 113-0033, Japan.

[2]Department of Biological Sciences, Graduate School of Science, The University of Tokyo, 7-3-1 Hongo, Bunkyo-ku, Tokyo 113-0033, Japan.

[3]Molecular Genetics Research Laboratory, Graduate School of Science, The University of Tokyo, 7-3-1 Hongo, Bunkyo-ku, Tokyo 113-0033, Japan.

[4]Department of Neurology, Fujita Health University School of Medicine, Toyoake 470-1192, Aichi, Japan.

[5]Lead contact

*Correspondence to: skuroda@bs.s.u-tokyo.ac.jp (S.K.)

Key words

Alzheimer's disease, multi-omics, trans-omics, network medicine, systems biology, energy metabolism

Abstract

Alzheimer's disease (AD), a leading cause of dementia, has been recognized as a disease with profound metabolic dysregulation. However, a systems-level view of metabolic regulation across multiple omic modalities in AD remains elusive. Here, we integrated public multi-omic datasets (transcriptome, proteome, and metabolome) from the dorsolateral prefrontal cortex of AD patients and controls. By leveraging existing molecular biological knowledge, we reconstructed a multi-layered metabolic regulatory network to systematically map the interplay between mRNAs, proteins, and metabolites in AD. Our analysis revealed a coordinated downregulation of energy producing pathways, including the TCA cycle, oxidative phosphorylation, and ketone body metabolism, driven by reduced enzyme abundance and inhibitory allosteric effects. In contrast, the glycolysis/gluconeogenesis pathway appeared to be influenced by opposing enzymatic and allosteric regulations. These findings highlight key metabolic dysregulations that may contribute to the bioenergetic deficits in AD pathology.

Introduction

Alzheimer's disease (AD) is a leading cause of dementia and affects tens of millions of people worldwide currently [2]. It is pathologically characterized by senile plaques, neurofibrillary tangles, and cerebral atrophy [1]. Many risk factors are involved in the development of this disease: aging, genetic factors, vascular disease, infections, environmental factors, and metabolic disorders [1].

Some studies have focused on the role of altered metabolism in AD. One well-known abnormality that appears early in the progression of dementia is downregulation of glucose metabolism [3]. In the clinical settings, fluorodeoxyglucose (FDG)-positron emission tomography (PET) is used to detect the changes in glucose metabolism in the brain and to distinguish between different types of dementia [4]. FDG-PET detects reduced glucose consumption in the parietal-temporal area, medial temporal lobes, and posterior cingulate cortices during early AD, which later extends to the frontal lobes and subcortical areas [5, 6]. One of the causes for the dysregulation of glucose metabolism is the downregulation of GLUT1 and GLUT3, glucose transporters involved in glucose uptake into brain tissue. These transporters are downregulated in AD patients [7, 8, 9], correlating with the extent of amyloid beta (Aβ) accumulation and neurofibrillary tangles [9, 10]. Mitochondrial dysfunction is another key feature of AD pathology [11]. Studies of postmortem brain tissue have revealed impairments in the pyruvate dehydrogenase complex (PDHC) [12] and mitochondrial respiratory chain complexes [13] in patients with AD compared to cognitively normal subjects. More recently, there has been growing interest in the link between type 2 diabetes mellitus and AD, because brain insulin resistance has been observed in AD brains. This pathology, defined as the failure of brain cells to respond to insulin, leads to synaptic dysfunction and impaired immune response [14, 15]. Together, these metabolic abnormalities result in bioenergetic deficits, oxidative stress, chronic inflammation, and protein quality control failures in AD [16].

Large-scale and multi-omic analyses have identified many genes, proteins, and metabolic pathways that are associated with AD [17, 18, 19]. For example, co-expression network analysis of brain proteomic data has identified protein network modules associated with microglia, astrocytes, and sugar metabolism as the most strongly altered in AD [20]. Integrative multi-omic network analysis has shown that short-chain acylcarnitines/amino acids and medium/long-chain acylcarnitines are most

associated with AD clinical outcomes, implicating regulatory roles of *ABCA1* and *CPT1A* [21]. More recently, machine learning techniques have been applied to the integration of multi-omic data and the identification of functional modules and key molecules related to AD [22, 23]. However, these studies predominantly focus on correlations and biomarkers rather than elucidating the details of the mechanistic regulation by the physicochemical interactions between the molecules belonging to different modalities.

"Trans-omic analysis" can be a powerful approach for reconstructing a cross-hierarchical molecular regulatory network by integrating comprehensive quantitative data of molecules measured at multiple levels (gene expression level, protein abundance, and metabolite abundance) with existing molecular biological knowledge. Such an approach has been applied to study obesity in mouse models and identify regulatory changes in metabolic reactions in the liver and muscle in either the fasting state or after glucose administration [24, 25, 26, 27].

Here, we reconstructed a trans-omic network to uncover regulatory changes in metabolic reactions between cognitively normal control subjects and AD patients. We used public multi-omic datasets (transcriptomic, proteomic, and metabolomic data) of the dorsolateral prefrontal cortex (DLPFC) from the Religious Order Study and the Memory and Aging Project (ROSMAP) study [28,29]. The metabolic trans-omic analysis revealed AD-associated dysfunction due to changes in enzyme abundance and allosteric regulation by metabolites in pathways related to energy production, such as the glycolysis/gluconeogenesis pathway, the TCA cycle, the oxidative phosphorylation pathway, and ketone body metabolism. These findings provide a systems-level insight into intracellular metabolic dysregulation that may underlie the pathology of AD.

Results

Overview of trans-omic analysis for metabolic reactions of Alzheimer's disease

To understand metabolic dysfunction in AD, we constructed a trans-omic network that integrated transcriptomic, proteomic, and metabolomic data from postmortem human brain tissue. We primarily used public multi-omic datasets [20,35,38] obtained from the DLPFC collected from cognitively normal individuals and patients with AD in the ROSMAP study [28,29]. Although pathological changes in AD are prominent in other areas like the temporal and parietal lobes, our study focused on the DLPFC due to the unique availability of comprehensive, matched multi-omic data for this region. The transcriptome was measured by bulk RNA sequencing (NGS), the proteome by tandem mass tag (TMT)-MS, and the metabolome by UPLC-MS/MS (Fig. 1).

We identified differentially expressed genes (DEGs), proteins (DEPs), and metabolites (DEMs) in AD patients compared to cognitively normal controls using each omic dataset (Fig. 1, Step 1). To focus on metabolic regulation, we used KEGG [30] and BRENDA [31] to match enzymes and metabolites to metabolic reactions and then determined AD-associated differences in metabolic regulation ("differential regulation") (Fig. 1, Step 2). We also identified the enzyme mRNAs and transcription factors (TFs) that may be involved in the metabolic changes in AD [43,44]. We then reconstructed a metabolic trans-omic network through integrating all these molecular relationships spanning multi-omic modalities (Fig. 1, Step 3). We further analyzed metabolic pathways in the trans-omic network related to energy production, including glycolysis/gluconeogenesis, the TCA cycle, oxidative phosphorylation, and ketone body metabolism (Fig. 1, Step 4).

Identification of differentially expressed molecules of AD

We accessed the omic data and associated clinical, demographic, and postmortem neuropathological data for each sample from the ROSMAP Study through the AD Knowledge Portal (https://adknowledgeportal.synapse.org/). A detailed summary of the samples used in this study, including the overlap across the three omics modalities, is provided in Fig. S1. To ensure the representativeness of this cohort, we compared the ROSMAP Study dataset with other public datasets or results from specific published studies (see also Fig. S2 and Methods section).

We defined the cognitively normal control (CT) group and the AD group based on

clinical diagnosis and neuropathological diagnoses (Braak Stage and CERAD score) (see also Fig. S1A and Methods section) [32,33].

We defined 946 significantly increased mRNAs and 917 decreased mRNAs in AD using the results of the differential expression analysis from the RNA-seq Harmonization Study [35] (Synapse id: syn8456721). We identified 657 significantly increased proteins and 854 decreased proteins in AD using the proteomic data in the ROSMAP Study (id: syn21266454) [20,37]. We identified 79 significantly increased metabolites and 78 decreased metabolites in AD using the metabolomic data from the ROSMAP study [38] (id: syn25985690).

We conducted enrichment analyses for each omic modality, confirming that our findings were consistent with previous studies (Fig. S3 and Supplementary text). Furthermore, we constructed protein-protein interaction networks for the increased and decreased DEPs using the STRING database [54] (Fig. S4). The result indicated a decrease in translation, both in the nucleus and in the mitochondria, suggesting that this translational dysregulation could have a crucial impact on the proteomic changes in AD. We also visualized the top 20 DEGs, DEPs, and DEMs with $\log_2$FC values (Fig. S5A, S5B, S5C, and Supplementary text). Of note, the abundance of ATP was not quantified in the metabolomic data from the ROSMAP study [38].

Relationship between proteomic changes and gene expression changes in AD

To examine the relationship between DEGs and DEPs, we investigated the expression changes of the genes encoding each DEP (Fig. S6A). Among the increased DEPs, 76 DEPs were encoded by significantly upregulated genes, and 15 DEPs were encoded by significantly downregulated genes. Among the decreased DEPs, 70 DEPs were encoded by genes with significantly decreased expression, and 12 DEPs were encoding by genes with significantly increased expression. Thus, many of the DEPs did not have coordinated expression changes with their encoding genes (Fig. S6B). This result is consistent with previous studies using postmortem human transcriptomic and proteomic data [37,42].

Identification of differentially expressed transcription factors

We identified TFs potentially involved in regulating the expression changes of the DEGs using ChIP-Atlas, a database that integrates and provides ChIP-seq data [43,44].

No TFs were predicted to regulate genes with significantly decreased expression; 19 TFs were identified as regulators of genes with significantly increased expression (Table S1). To determine the TFs with differential activity in AD, we investigated whether the predicted TFs were encoded by DEGs or were DEPs (Fig. S6C). We identified five TFs that were significantly increased at either the transcriptomic level (CTCF, MAX, and ZNF143) or the proteomic level (BRD4 and RAD21). We defined these 5 TFs as "differentially expressed transcription factors" (DETFs). Recent findings have shown the protective role of BRD4, which inhibits transcriptional expression of AD-related genes [60,61,62].

Identification of metabolic enzymes among the differentially expressed proteins

To focus on the proteomic changes in AD that are relevant to cellular metabolism, we identified metabolic enzymes among the DEPs according to their designations as metabolic enzymes in the "Metabolic pathways" of the KEGG PATHWAY Database [30]. Among the 657 significantly increased proteins, 59 are metabolic enzymes. Among the 854 significantly decreased proteins, 70 are metabolic enzymes (Table S2).

Identification of metabolites that are substrates, products, or allosteric regulators of metabolic reactions

Metabolic reactions are regulated not only by the abundance of the metabolic enzymes that catalyze the reactions, but also by the abundance of substrates and products, as well as by allosteric regulators. Using the BRENDA database [31], we identified allosteric regulators among the DEMs: 46 were increased in AD and 26 were decreased in AD (Fig. 2A). These 72 allosteric regulatory DEMs affected 318 enzymes. Using the KEGG REACTION database [30], we also identified substrates and products of metabolic reactions among the DEMs: 50 substrates or products were increased in AD and 33 were decreased in AD, affecting 727 enzymes (Fig. 2B).

Construction of a trans-omic network for differentially regulated metabolic reactions

We constructed a metabolic trans-omic network for differentially regulated metabolic reactions in AD (Fig. 2C and Supplementary Data 1). This network integrates five interconnected components organized into corresponding layers: (1) DETFs in the "TF

layer", (2) DEGs encoding metabolic enzymes in the "Enzyme mRNA layer", (3) DEPs functioning as metabolic enzymes in the "Enzyme Protein layer", (4) metabolic reactions differentially regulated by enzymes or metabolites in the "Metabolic Reaction layer", and (5) DEMs involved in the metabolic reactions as allosteric regulators, products, or substrates in the "'Metabolite layer". The adjacent layers are connected by edges based on the regulatory relationships between the molecules. The right panel of Fig. 2C shows the schema for the construction of the trans-omic network, corresponding to the five layers in the left panel. Specifically, the interlayer connections from the "Metabolite layer" to the "Metabolic Reaction layer" consisted of regulatory connections mediated by allosteric regulators, substrates, or products of each metabolic reaction [24,25,26]. Activating regulation of metabolic reactions is shown as red arrows, and inhibiting regulation is shown as blue arrows (see also Fig. S7, and Methods section).

We analyzed the degree centrality of nodes in the metabolic reaction network that consisted of "Enzyme Protein layer", "Metabolic Reaction layer", and "Metabolite layer." Degree centrality is a measure of the importance of a node in network theory [45]. The degree centrality of a node is calculated by normalizing the number of edges connected to that node, with a higher value indicating greater influence within the network. AMP, which increased in the AD group, had the highest degree centrality (Fig. 2D). Glutamate and 2-oxoglutarate (α-ketoglutarate), both of which increased in the AD group, were second and third in degree centrality, respectively. Acetyl-CoA, which decreased in the AD group, ranked fourth.

The metabolic dysregulations of energy metabolic pathways of AD

We extracted key metabolic pathways involved in energy production in the trans-omic network, the glycolysis/gluconeogenesis pathway, the TCA cycle, oxidative phosphorylation, and ketone body metabolism. We examined detailed metabolic dysregulation in each pathway (Fig. 3, Fig. S7).

In the glycolysis/gluconeogenesis pathway, increased expression of TPI1, GAPDH, PGAM2, ENO1, and PKM would increase flux through the glycolysis/gluconeogenesis pathway, whereas the increased metabolites S7P, AMP, threonine, alanine, tyrosine, valine, urea, glutamate, and phenylalanine would allosterically inhibit flux through the pathway. In addition, the expression of GLUT3, a transporter responsible for the basal

uptake of glucose in neurons [46], is significantly decreased (Fig. 3A), as demonstrated in several previous studies [8,9,10]. However, the mRNA expression of *GLUT3* did not show a significant change in AD.

Previous studies have reported downregulation of PDHC in AD patients [47,48]. Consistently, we found that five of the six proteins comprising the complex, PDHA1, PDHB, PDHX, DLD and DLAT, were significantly decreased. In addition, acetyl-CoA, was significantly decreased in AD. The previous studies [47, 48] and our findings suggest that reduced PDHC activity may decrease the production of acetyl-CoA in AD.

In the TCA cycle, most regulations were inhibitory (Fig. 3B). Three metabolic enzymes were significantly decreased: SDHA, CS, and IDH2. Increases in AMP, glutamate, and maleic acid resulted in allosteric inhibition of metabolic reactions in the TCA cycle. Only a reduction in nicotinamide D-ribonucleotide exhibited an allosteric activating effect. Among the five measured metabolites (citrate, aconitate, 2-oxoglutarate, fumarate, and malate) that are substrates and products in the TCA cycle, 2-oxoglutarate (α-ketoglutarate) showed a significant increase in abundance.

In oxidative phosphorylation, most of the regulatory changes in AD resulted in inhibition of metabolic reactions (Fig. 3C). Five subunits of complex I in the respiratory chain were decreased: NDUFS8, NDUFS7, NDUFV1, NDUFS1, and MT-ND3. This result is consistent with other postmortem studies of human brains which have shown reduced expression of genes encoding subunits of the electron transport chain in posterior cingulate cortex, middle temporal gyrus, and the hippocampus of AD patients [49]. The activity of complex II was also negatively impacted by the decrease in SDHA and an increase in the allosteric inhibitor, maleic acid. The increase in phenylalanine, an allosteric regulator of complex V, provided the only activating regulation.

Ketone bodies are the second-most utilized energy source in the brain after glucose [50]. Ketone bodies are synthesized in the liver in the form of 3-hydroxybutyrate and acetoacetate, which are transported to the brain through the circulation [50]. Ketone bodies undergo several metabolic reactions and are converted to acetyl-CoA as an energy source in mitochondria [50]. Most of the AD-associated changes resulted in inhibition of ketone body metabolism (Fig. 3D). Among the metabolic enzymes involved in ketone body metabolism, BDH1, HMGCL, and HMGCS1 were downregulated; only ACAT2 was upregulated. The increase in glutarate and AMP resulted in inhibitory allosteric regulation. Collectively, these results suggested that

reduced ketone body metabolism contributed to the decrease in acetyl-CoA abundance in AD.

Through this examination of the changes in the regulation of core metabolic pathways involved in energy production, we found antagonistic regulation by enzymes and allosteric regulators in the glycolysis/gluconeogenesis pathway. On the other hand, the TCA cycle, oxidative phosphorylation, and ketone body metabolism were downregulated in AD due to the reduced enzymes and inhibitory allosteric effects. Here, we demonstrate the systems-level of the dysregulated energy production of AD in terms of the metabolic trans-omic network.

Discussion

In this study, we identified differentially expressed molecules from public datasets of transcriptome, proteome, and metabolome obtained from the ROSMAP study and used the results to construct a metabolic trans-omic network for differentially regulated metabolic reactions in AD. We then performed a detailed analysis of the AD-associated changes in pathways related to energy production.

Several key factors that underlie the mechanism of dysregulated energy metabolism have been identified by many previous studies [3,7,8,9,10,11,12,13,14,15], including downregulated glucose uptake and utilization, impaired mitochondrial functions, dysfunctional enzyme proteins, and brain insulin resistance, among others. However, details of the regulatory relationships between the molecules belonging to different modalities have been poorly understood. Here, we demonstrated a potential mechanistic picture of dysregulated core energy metabolism in AD (Fig. 4): (1) inhibition of the TCA cycle, oxidative phosphorylation, and ketone body metabolism by allosteric inhibition and downregulated enzyme proteins, (2) antagonistic regulation by enzymes and allosteric regulators in the glycolysis/gluconeogenesis pathway.

As previously reported [59], mitochondrial dysfunction accompanies the progression of AD, which may lead to downregulation of TCA cycle, oxidative phosphorylation and ketone body utilization pathways, since these metabolic reactions occur within mitochondria. Additionally, decreased expression of the subunit proteins that make up PDHC and allosteric inhibition to the glycolysis pathway may further reduce acetyl-CoA levels, resulting in a greater decrease in the ability to produce enough ATP. This energetic shortage appears to be partially compensated by upregulation of glycolytic enzymes, but this compensatory mechanism could be inhibited by the reduced glucose uptake through GLUT3 in neurons. Previous studies have also suggested an upregulated glycolysis pathway in astrocytes as a compensatory mechanism to provide the energy source for impaired neurons during AD progression [63].

The DEM analysis revealed significant increases in 12 amino acids (Glu, Tyr, Thr, Phe, Asn, Ser, Arg, Val, Leu, Ala, Met, and Lys), 2-oxoglutarate, and urea. In addition, we identified ASL, an enzyme involved in the urea cycle [51], as significantly increased in AD. Thus, our results highlighted the potential involvement of nitrogen metabolism dysregulation in AD and suggested that the observed accumulation of urea may result from enhanced flux through the urea cycle within the DLPFC. This could reflect a response to elevated amino acids levels, potentially linked to compromised translation and protein turnover. This hypothesis is also supported by the results of our PPI network

analysis and the low correlation between mRNA expression and protein expression.

Previous studies have demonstrated that transcripts of ribosomal proteins are significantly downregulated in the dentate gyrus in AD patients [53]. In another recent research, changes in the proteome are important for understanding AD pathology, because approximately half of the network modules identified in protein networks were not found in RNA networks [37]. About nitrogen metabolism in AD, a previous study has demonstrated that astrocytic urea metabolism induced in AD exhibits a beneficial effect on Aβ detoxification. However, this metabolic process has been found to induce memory impairment through producing toxic byproducts, ammonia and H_2O_2, and GABA [52].

We summarized the metabolic dysregulations observed in the brain of AD (Fig. 4). Collectively, our data suggests that preserving or improving the ability to produce ATP and early intervention in the process of nitrogen metabolism are candidates for the prevention and treatment of dementia.

Limitations of this study

Our analysis did not distinguish between cell types. Brain tissue contains various types of cells: neurons, astrocytes, oligodendrocytes, and microglia. The genes and proteins expressed in each cell type differ, as do the metabolic reactions that occur within each cell [55,56]. A previous study has reported that Braak stage negatively correlated with the proportion of oligodendrocytes and positively correlated with the proportions of microglia and astrocytes [57,58]. Therefore, our results could partly reflect changes in tissue composition associated with the progression of AD. A recent study using the snRNA-seq technique has demonstrated that in excitatory neurons downregulated DEGs that were correlated with NFT burden were enriched for TCA cycle. In addition, the glycolysis and oxidative phosphorylation modules were upregulated in astrocytes and microglia in AD group [64]. In future research, further advancements in technologies that enable the acquisition of proteomic and metabolomic data at the single-cell level are anticipated.

All omics data used in this study were measured from postmortem brain tissues. The cause of death and events that occur immediately before death (such as resuscitation) can influence molecular profiles of postmortem tissue. Thus, we must consider potential biases related to these factors.

In this study, we analyzed the DLPFC because that was the region with sufficient datasets. However, initial pathological changes of AD typically appear in the medial

temporal lobe. Therefore, trans-omic analyses should also be conducted in this region. It is also possible that the results of this study reflect changes that compensate for metabolic alterations arising in other regions. However, at present, the number of large-scale proteomic and metabolomic datasets measured from human postmortem brains is limited. It is anticipated that future research will involve large-scale omics measurements spanning multiple brain regions, such as spatial transcriptomic and proteomic analyses.

1 **Main figures**

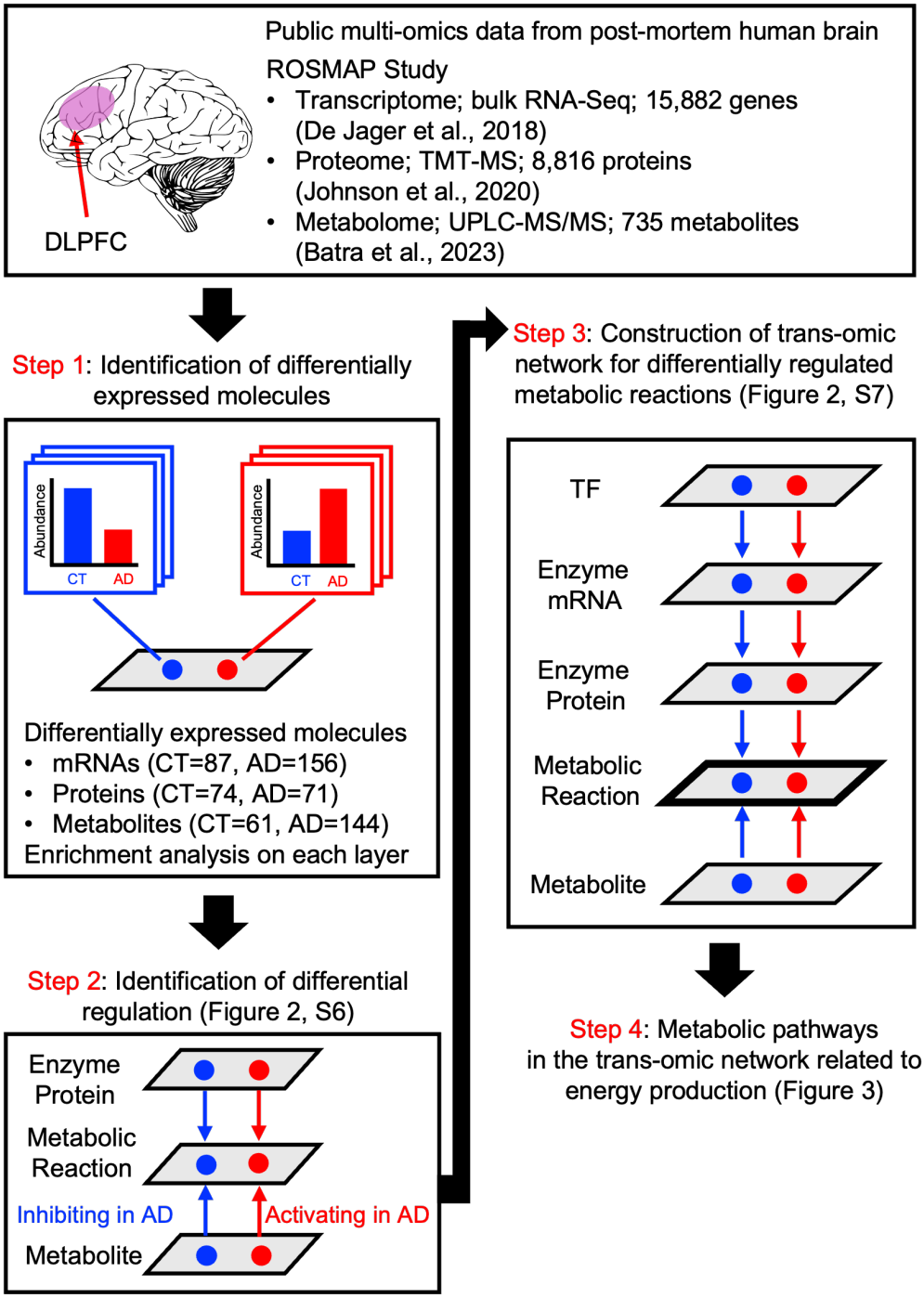

2

3 **Figure 1. Overview of trans-omic analysis for metabolic reactions in Alzheimer's**
4 **disease**

5 The illustration shows how public multi-omic data from the DLPFC of cognitively
6 normal subjects (CT) and patients with Alzheimer's disease (AD) from the ROSMAP
7 study [28,29] were used to generate a metabolic trans-omic network (Steps 1-3) and to

perform detailed analysis of energy production pathways (Step 4). Red indicates differentially expressed molecules with increased expression or abundance, regulatory events that activate metabolic reactions, or increased activity of a metabolic reaction. Blue indicates differentially expressed molecules with decreased expression or abundance, regulatory events that inhibit metabolic reactions, or reduced activity of a metabolic reaction. The sample size for each analysis: n = 87 (CT group) and n = 156 (AD group) for transcriptomics, n = 74 (CT group) and n = 71 (AD group) for proteomics, and n = 61 (CT group) and n = 144 (AD group) for metabolomics.

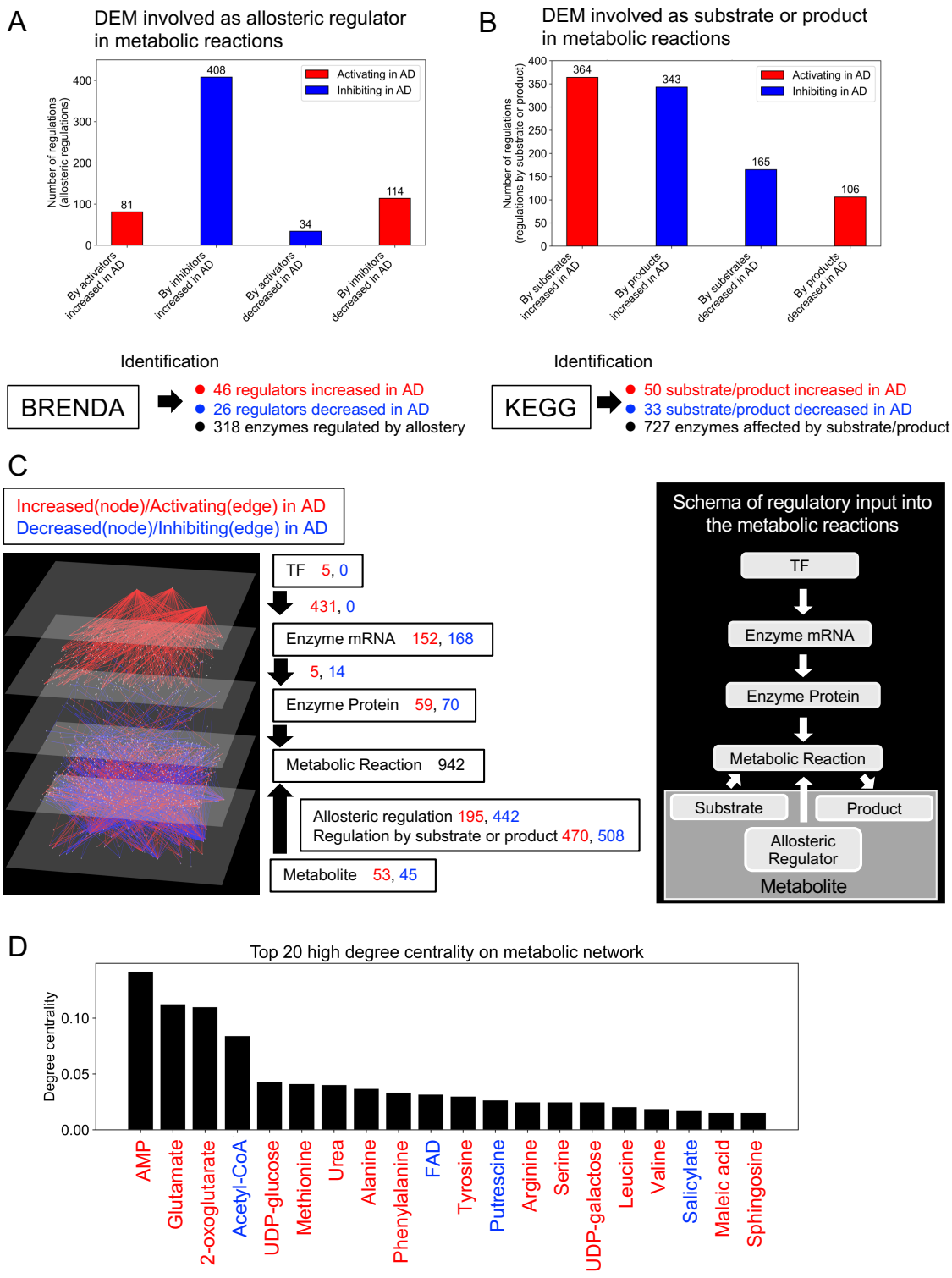
A
DEM involved as allosteric regulator in metabolic reactions
Number of regulations (allosteric regulations)
Activating in AD
Inhibiting in AD
81
408
34
114
By activators increased in AD
By inhibitors increased in AD
By activators decreased in AD
By inhibitors decreased in AD
B
DEM involved as substrate or product in metabolic reactions
Number of regulations (regulations by substrate or product)
364
343
165
106
By substrates increased in AD
By products increased in AD
By substrates decreased in AD
By products decreased in AD
Identification
BRENDA
46 regulators increased in AD
26 regulators decreased in AD
318 enzymes regulated by allostery
Identification
KEGG
50 substrate/product increased in AD
33 substrate/product decreased in AD
727 enzymes affected by substrate/product
C
Increased(node)/Activating(edge) in AD
Decreased(node)/Inhibiting(edge) in AD
TF 5, 0
431, 0
Enzyme mRNA 152, 168
5, 14
Enzyme Protein 59, 70
Metabolic Reaction 942
Allosteric regulation 195, 442
Regulation by substrate or product 470, 508
Metabolite 53, 45
Schema of regulatory input into the metabolic reactions
TF
Enzyme mRNA
Enzyme Protein
Metabolic Reaction
Substrate
Product
Allosteric Regulator
Metabolite
D
Top 20 high degree centrality on metabolic network
Degree centrality
AMP
Glutamate
2-oxoglutarate
Acetyl-CoA
UDP-glucose
Methionine
Urea
Alanine
Phenylalanine
FAD
Tyrosine
Putrescine
Arginine
Serine
UDP-galactose
Leucine
Valine
Salicylate
Maleic acid
Sphingosine

Figure 2. Construction of a trans-omic network for differentially regulated metabolic reactions

(A) The number of allosteric regulators among DEMs and the number of allosteric regulations mediated by them on metabolic enzymes identified with BRENDA. Some reactions are regulated by more than one DEM and some DEMs regulate multiple enzymes, thus the number of regulations exceeds the number of enzymes identified with BRENDA and the number of DEMs.

(B) The number of substrates or products among DEMs and the number of regulations by them on metabolic enzymes identified with KEGG. Some reactions involve multiple substrates or yield multiple products and some substrates and products occur in multiple reactions, thus the number of regulations exceeds the number of enzymes identified with KEGG and the number of DEMs.

(C) The trans-omic network for differentially regulated metabolic reactions (left). Nodes and edges indicate differentially expressed molecules and differential regulations involved in metabolic reactions, respectively. Schema of regulatory input into the metabolic reactions (right). TFs control metabolic enzyme mRNA abundance through gene regulation. Metabolite acts as substrates, products, and allosteric regulators in metabolic reactions.

(D) Top 20 molecules with high degree centrality on the metabolic network. The metabolic network consisted of the nodes and edges from the “Enzyme Protein”, “Metabolic Reaction”, and “Metabolite” layers of the trans-omic network. Those shown in red text were increased in AD; those in blue were decreased in AD.

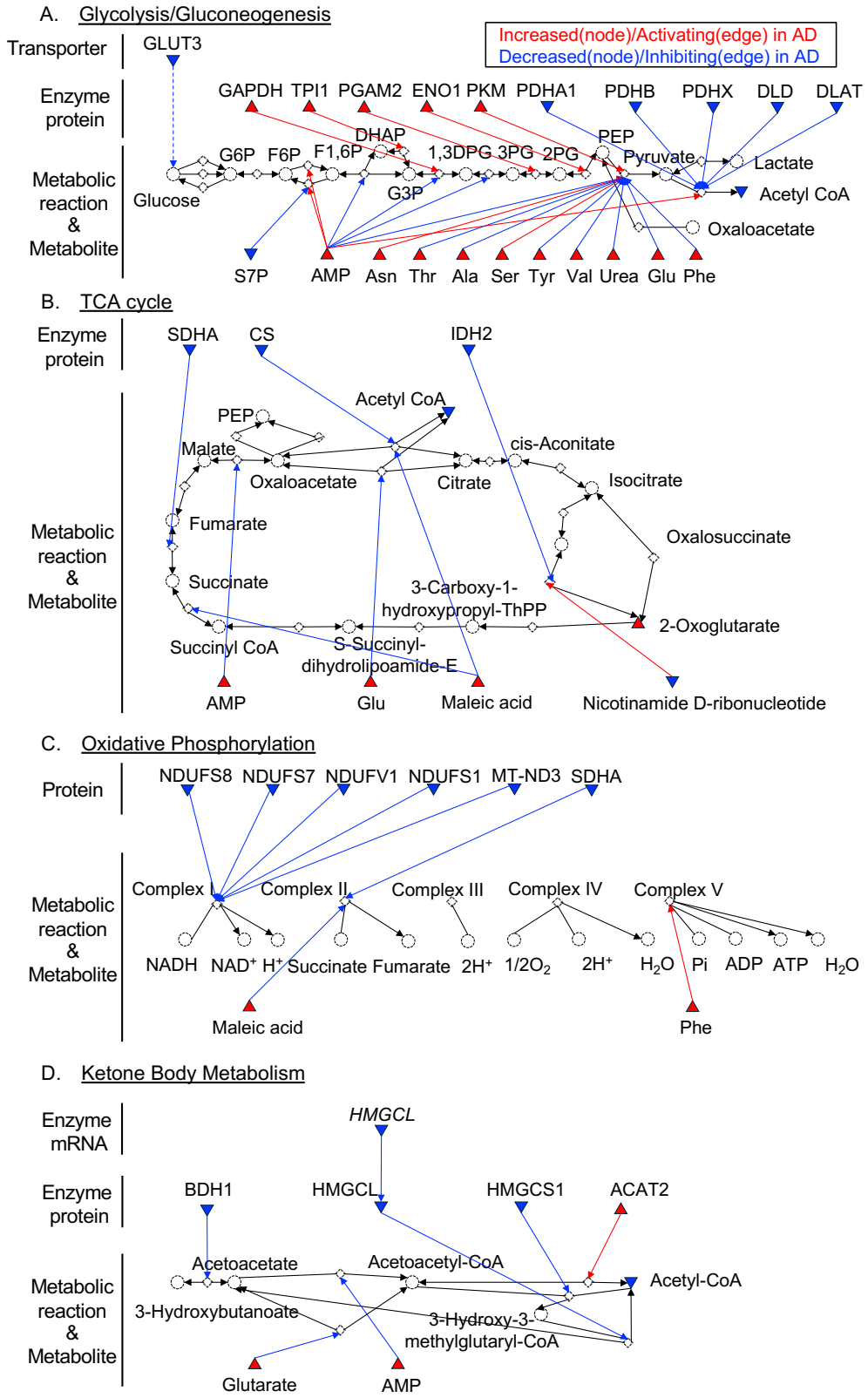
A. Glycolysis/Gluconeogenesis
Increased(node)/Activating(edge) in AD
Decreased(node)/Inhibiting(edge) in AD
Transporter
GLUT3
Enzyme protein
GAPDH TPI1 PGAM2 ENO1 PKM PDHA1 PDHB PDHX DLD DLAT
Metabolic reaction & Metabolite
Glucose
G6P F6P F1,6P DHAP 1,3DPG 3PG 2PG PEP Pyruvate
G3P
Lactate
Acetyl CoA
Oxaloacetate
S7P AMP Asn Thr Ala Ser Tyr Val Urea Glu Phe
B. TCA cycle
Enzyme protein
SDHA CS IDH2
Metabolic reaction & Metabolite
Acetyl CoA
PEP
Malate
Oxaloacetate
Citrate
cis-Aconitate
Isocitrate
Fumarate
Oxalosuccinate
Succinate
3-Carboxy-1-hydroxypropyl-ThPP
2-Oxoglutarate
Succinyl CoA
S-Succinyl-dihydrolipoamide-E
AMP Glu Maleic acid Nicotinamide D-ribonucleotide
C. Oxidative Phosphorylation
Protein
NDUFS8 NDUFS7 NDUFV1 NDUFS1 MT-ND3 SDHA
Metabolic reaction & Metabolite
Complex I Complex II Complex III Complex IV Complex V
NADH NAD+ H+ Succinate Fumarate 2H+ 1/2O2 2H+ H2O Pi ADP ATP H2O
Maleic acid
Phe
D. Ketone Body Metabolism
Enzyme mRNA
HMGCL
Enzyme protein
BDH1 HMGCL HMGCS1 ACAT2
Metabolic reaction & Metabolite
Acetoacetate
Acetoacetyl-CoA
Acetyl-CoA
3-Hydroxybutanoate
3-Hydroxy-3-methylglutaryl-CoA
Glutarate AMP

Figure 3. The metabolic dysregulations of energy metabolic pathways of AD

The trans-omic changes in the regulations of glycolysis/gluconeogenesis (A), TCA cycle (B), oxidative phosphorylation (C), and ketone body metabolism (D). The information for each pathway were obtained from "glycolysis/gluconeogenesis" (hsa00010), "TCA cycle" (hsa00020), "oxidative phosphorylation" (hsa00190), and "butanoate metabolism" (hsa00650) in the KEGG database. Red upward triangles, increased molecules in AD; blue downward triangles, decreased molecules in AD. Red arrow, regulations that activate metabolic reactions; blue arrow, regulations that inhibit reactions. Unfilled circles with dashed outlines represent molecules that were not differentially expressed or were not measured. Unfilled diamond nodes with dashed outlines represent metabolic reactions. See Fig. S7 and Methods section for additional details.

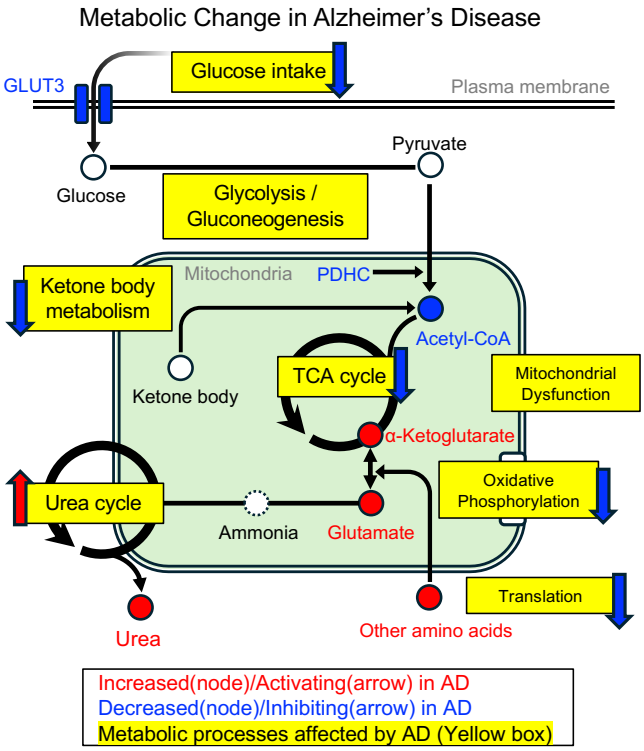

Figure 4. Models of potentially dysregulated metabolic processes in AD

Diagrams of dysregulated metabolic pathways associated with the progression of AD. Metabolic processes affected by AD are highlighted in yellow boxes. Red, increased (circles) or activating (arrows) in AD; blue, decreased (circles and GLUT3) or inhibiting (arrows) in AD.

Materials & methods

ROSMAP study

Public multi-omic datasets measured from postmortem human brain samples from the Religious Orders Study and Memory and Aging Project (ROSMAP) study were used in this study. (https://adknowledgeportal.synapse.org/Explore/Studies/DetailsPage/StudyDetails?Study=syn3219045#StudyDescription) [27,28]. All data were obtained through the AD Knowledge Portal (https://adknowledgeportal.synapse.org/). The Religious Orders Study (ROS) and the Memory and Aging Project (MAP) are long-term studies that focus on memory, motor function, and functional problems in older adults. ROS includes Catholic nuns, priests, and brothers aged 65 and older; MAP includes older adults around Chicago. Both studies include annual clinical assessments, self-reports, and postmortem brain donations. Diagnosis of dementia is made using the same procedure in both studies, and final clinical diagnosis and pathological assessment are made after death. Further details of the studies can be found in [27,28].

RNA sequencing

For transcriptomic data, the results of differential expression analysis from the RNAseq Harmonization Study [35] were used. For detailed methods of RNA-seq and differential expression analysis, see (https://adknowledgeportal.synapse.org/Explore/Studies/DetailsPage/StudyDetails?Study=syn3219045#Methods-GeneExpressionRNAseq) and (https://adknowledgeportal.synapse.org/Explore/Studies/DetailsPage/StudyDetails?Study=syn9702085#StudyDescription).

Proteomic analysis

For the proteomic data, proteomic analysis in the ROSMAP study were used [20,37]. In that study, brain tissue samples from the ROSMAP cohort (n = 400) were tagged using the TMT 10-plex kit. Further details of the TMT-MS experiment are available at (https://adknowledgeportal.synapse.org/Explore/Studies/DetailsPage/StudyDetails?Study=syn3219045#Methods-ProteomicsTMTquantitation). For information on batch effect correction, outlier and covariate adjustment of the raw data, refer to [20,37].

Metabolomic analysis

For metabolomic data, UPLC-MS/MS analysis in the ROSMAP Study was used, which

were generated at Metabolon and preprocessed by the Alzheimer's Disease Metabolomics Consortium [38]. Further details of the UPLC-MS/MS experiments and data normalization can be found at (https://adknowledgeportal.synapse.org/Explore/Studies/DetailsPage/StudyDetails?Study=syn3219045#Methods-MetabolomicsMetabolonHD4).

Validation analysis

To ascertain how the choice of the ROSMAP Study as the data source could influence our analyses, the ROSMAP Study data were compared with other datasets or findings from specific published studies (Fig. S2). For validation of transcriptomic data, RNA-seq data from the Mount Sinai Brain Bank (MSBB) Study was used (https://www.synapse.org/Synapse:syn10526259) [34]. For validation of proteomic data, TMT-MS results from the Accelerating Medicines Partnership Alzheimer's Disease Diverse Cohorts Study (AMP-AD DiverseCohorts) were used ((https://adknowledgeportal.synapse.org/Explore/Studies/DetailsPage/StudyDetails?Study=syn51732482#Methods-ProteomicsTMTquantitation). A reasonable correlation (correlation coefficient 0.53) between the gene expression (transcriptomic) data from the ROSMAP Study and MSBB Study, and between the proteomic data from the ROSMAP Study and the AMP-AD DiverseCohorts (correlation coefficient 0.60) was obtained.

Definition of CT group and AD group

The CT group consisted of subjects whose clinical diagnosis was categorized as "No cognitive impairment", with a Braak Stage of III or lower and a CERAD score indicating "no AD" or "possible AD". The AD group comprised subjects whose clinical diagnosis was categorized as "Alzheimer's dementia and no other cause of cognitive impairment", with a Braak Stage of IV or higher and a CERAD score indicating "probable AD" or "definite AD".

Identification of differentially expressed molecules between CT and AD

To define the differentially expressed genes (DEGs) in AD compared to CT, the results of the differential expression analysis from the RNA-seq Harmonization Study were used (https://www.synapse.org/Synapse:syn8456721). In the study, the adjusted p-value and log2FC value of each gene in the two groups were calculated using the count data from RNA sequencing of postmortem brains (DLPFC) from 634 subjects (156 AD and

87 CT) in the ROSMAP Study. The values were calculated after adjusting for covariates such as age, gender, post-mortem interval (PMI), and RNA integrity number (RIN) score using the voom-limma package in R. In that analysis, genes with an adjusted p-value < 0.05 were defined as DEGs.

To identify the DEPs in AD compared to CT, the log2-transformed and normalized relative quantitative data (https://www.synapse.org/Synapse:syn21266454) measured by isobaric tandem mass tagging peptide labeling in the ROSMAP study (71 AD and 74 CT) were used. Following the exclusion of proteins with more than 50% missing values, ANCOVA was performed with gender and PMI as covariates for the remaining 8,816 proteins. Subsequently, the q-value and log2FC were calculated using the Storey's method. Proteins with a q-value < 0.05 were defined as DEPs.

To identify the DEMs in AD compared to CT, the normalized quantified data (https://www.synapse.org/Synapse:syn25985690) measured using UPLC-MS/MS in the ROSMAP Study (144 AD and 61 CT) were used. Following the exclusion of metabolites with more than 50% missing values, ANCOVA was performed with gender and PMI as covariates for the remaining 735 metabolites. Subsequently, the q-value and log2FC were calculated using the Storey's method. Metabolites with q-values < 0.05 were defined as DEMs.

Enrichment analysis

Enrichment analyses were conducted on DEGs and DEPs using Metascape (version 3.5; https://metascape.org/gp/index.html#/main/step1) [36]. Enrichment analysis was conducted on DEMs using MetaboAnalyst (version 6.0; https://www.metaboanalyst.ca/) [39]. The default settings were used for both analyses. The background was defined as all genes for proteomic analysis, and all metabolites from SMPDB for metabolomic analysis set as default in each software.

Inference of transcription factors for differentially expressed genes in DLPFC of AD

To infer the TFs involved in regulating the DEGs, we used the peak call data (TSS±1k) from ChIP-Atlas (https://chip-atlas.org/) [43,44]. The "neural" cell type was selected, and a threshold of 200 was applied for the statistical significance calculated by MACS2. The p-value was calculated using Fisher's exact test, and the Benjamini-Hochberg (BH) method was employed for FDR correction (q-value < 0.05).

Construction of protein-protein interaction networks

In constructing the protein-protein interaction network (Fig. S4A, S4B), we included protein pairs with a score of 400 or more in the STRING data [54] as interacting pairs. We constructed the protein-protein interaction network by connecting interacting DEPs with edges.

Construction of Trans-omic network for differentially regulated metabolic reactions

DEPs and transcripts were matched using the Ensembl protein ID [41]. Among the DEPs, proteins that were categorized as metabolic enzymes in the “metabolic pathways” of the KEGG PATHWAY database [30] were identified. Using BRENDA [31], the allosteric regulators belonging to DEMs were identified. Using KEGG REACTION data, the DEMs that are involved as substrates or products in metabolic reactions were identified. By integrating the above information, we identified DEPs that act as metabolic enzymes, the metabolic reactions in which they are involved, and the DEGs encoding these proteins, as well as DEMs and the metabolic reactions in which these metabolites are involved as allosteric regulators or as products or substrates. To identify DETFs in AD, we examined which the inferred TFs were encoded by DEGs or appeared as the DEPs. All these data were used to construct a 5-layered (DETFs, DEGs, DEPs, metabolic reactions, DEMs) trans-omic network for metabolic reactions in the DLPFC of AD patients.

The adjacent layers are connected by edges based on the regulatory relationships between the molecules on these layers. The “Enzyme mRNA” and “TF” layers were connected by red edges when mRNA expression increased and by blue edges when it decreased. The “Enzyme mRNA” and “Enzyme Protein” layers were connected by red edges when both gene and protein expression of enzymes increased, and by blue edges when gene and protein expression of enzymes decreased. The “Enzyme Protein” and “Metabolic Reaction” layers were connected by red edges when enzyme expression increased, and by blue edges when enzyme expression decreased. For the connection between "Metabolic Reaction” and “Metabolite” layer, if a metabolite shows an increase in expression and also has an allosteric effect of activating the metabolic reaction it controls, it is colored red; if it shows an increase in expression and also has an allosteric effect of inhibiting the metabolic reaction it controls, it is colored blue; if it shows a decrease in expression and also has an allosteric effect of activating the metabolic reaction it controls, it is colored blue; if it shows a decrease in expression and also has an allosteric effect of inhibiting the metabolic reaction it controls, it is colored red. If a metabolite shows an increase in expression and it is a substrate of the metabolic

reaction, it is colored red; if it shows an increase in expression and it is a product of the metabolic reaction, it is colored blue; if it shows an decrease in expression and it is a substrate of the metabolic reaction, it is colored blue; if it shows an decrease in expression and it is a product of the metabolic reaction, it is colored red.

Implementation

Statistical tests were performed using MATLAB 2023b (The Mathworks Inc; https://www.mathworks.com/products/matlab.html). Trans-omic network analysis and visualization were implemented in Python (version 3.12.2; https://www.python.org/), Pandas (version 1.5.3; https://pandas.pydata.org/) [65], Networkx (version 3.1; https://networkx.org/) [66], and Matplotlib (version 3.7.1; https://matplotlib.org/) [67] packages.

Resource availability

Lead contact

Further information and requests for resources and reagents should be directed to and will be fulfilled by the Lead Contact, Shinya Kuroda (skuroda@bs.s.u-tokyo.ac.jp).

Materials availability

This study did not generate any new material.

Data availability

All raw omics data used for this study are available through the AD Knowledge Portal (https://adknowledgeportal.org). The AD Knowledge Portal is a platform for accessing data, analyses, and tools generated by the Accelerating Medicines Partnership (AMP-AD) Target Discovery Program and other National Institute on Aging (NIA)-supported programs to enable open-science practices and accelerate translational learning. The data, analyses and tools are shared early in the research cycle without a publication embargo on secondary use. Data are available for general research use according to the following requirements for data access and data attribution (https://adknowledgeportal.synapse.org/Data%20Access).

Code availability

We utilized and modified the algorithm that was developed in our previous study, iTraNet [27]. The code used for the analysis in this paper is available upon request.

Acknowledgements

We thank Takashi Iwatsubo (The University of Tokyo), Kenichiro Sato (The University of Tokyo), Tadafumi Kato (Juntendo University), Yugi Katsuyuki (RIKEN), Junichi Maruyama (RIKEN), Kentaro Tomii (AIST), and Hafumi Nishi (Tohoku University), Tatsuhiko Tsunoda (The University of Tokyo) for valuable suggestions and discussions. We also thank our laboratory members for critically reading this manuscript.

This study was supported by the Japan Society for the Promotion of Science (JSPS) KAKENHI (JP21H04759), CREST, the Japan Science and Technology Agency (JST) (JPMJCR2123), and by The Uehara Memorial Foundation. K.M. receives funding from a Grant-in-Aid for Early-Career Scientists (JP21K15342). H.W. was supported by AMED Grant Number JP21wm0425016.

The results published here are in whole or in part based on data obtained from the AD Knowledge Portal (https://adknowledgeportal.org/).

For the transcriptome data, we used the results of differential expression analysis based on RNA-seq measurements from ROSMAP participants as part of the RNA-seq Harmonization Study (https://www.synapse.org/Synapse:syn8456721). We utilized proteome data obtained from participants of the ROSMAP Study (https://www.synapse.org/Synapse:syn21266454). We used metabolome data acquired from ROSMAP Study participants (https://www.synapse.org/Synapse:syn25985690).

For validation of transcriptome data, we used the results of a differential expression analysis conducted using the same method on RNA-seq data from The Mount Sinai Brain Bank (MSBB) Study within the same research (https://www.synapse.org/Synapse:syn10526259). For validation of proteome data, we used the TMT-MS results from The Accelerating Medicines Partnership Alzheimer's Disease Diverse Cohorts Study (AMP-AD_DiverseCohorts) (https://adknowledgeportal.synapse.org/Explore/Studies/DetailsPage/StudyDetails?Study=syn51732482#Methods-ProteomicsTMTquantitation).

We used ChatGPT and DeepL for the assistance of manuscript editing and coding.

The authors thank Nancy R. Gough (BioSerendipity, LLC) for editorial assistance and critical input.

Author contributions

T.K. and S.K. conceived and supervised the project; T.K. and H.S. analyzed the data; writing group consisted of T.K., K.M., H.S., H.W., and S.K.

Declaration of interests

The authors declare no competing interests.

References

1. Breijyeh, Z., & Karaman, R. (2020). Comprehensive Review on Alzheimer's Disease: Causes and Treatment. *Molecules (Basel, Switzerland)*, *25*(24), 5789. https://doi.org/10.3390/molecules25245789
2. Scheltens, P., De Strooper, B., Kivipelto, M., Holstege, H., Chételat, G., Teunissen, C. E., Cummings, J., & van der Flier, W. M. (2021). Alzheimer's disease. *Lancet (London, England)*, *397*(10284), 1577–1590. https://doi.org/10.1016/S0140-6736(20)32205-4
3. Yan, X., Hu, Y., Wang, B., Wang, S., & Zhang, X. (2020). Metabolic Dysregulation Contributes to the Progression of Alzheimer's Disease. *Frontiers in neuroscience*, *14*, 530219. https://doi.org/10.3389/fnins.2020.530219
4. de la Monte, S. M., & Tong, M. (2014). Brain metabolic dysfunction at the core of Alzheimer's disease. *Biochemical pharmacology*, *88*(4), 548–559. https://doi.org/10.1016/j.bcp.2013.12.012
5. Mosconi, L., Mistur, R., Switalski, R., Tsui, W. H., Glodzik, L., Li, Y., Pirraglia, E., De Santi, S., Reisberg, B., Wisniewski, T., & de Leon, M. J. (2009). FDG-PET changes in brain glucose metabolism from normal cognition to pathologically verified Alzheimer's disease. *European journal of nuclear medicine and molecular imaging*, *36*(5), 811–822. https://doi.org/10.1007/s00259-008-1039-z
6. Szablewski L. (2021). Brain Glucose Transporters: Role in Pathogenesis and Potential Targets for the Treatment of Alzheimer's Disease. *International journal of molecular sciences*, *22*(15), 8142. https://doi.org/10.3390/ijms22158142
7. Kyrtata, N., Emsley, H. C. A., Sparasci, O., Parkes, L. M., & Dickie, B. R. (2021). A Systematic Review of Glucose Transport Alterations in Alzheimer's Disease. *Frontiers in neuroscience*, *15*, 626636. https://doi.org/10.3389/fnins.2021.626636
8. Simpson, I. A., Chundu, K. R., Davies-Hill, T., Honer, W. G., & Davies, P. (1994). Decreased concentrations of GLUT1 and GLUT3 glucose transporters in the brains of patients with Alzheimer's disease. *Annals of neurology*, *35*(5), 546–551. https://doi.org/10.1002/ana.410350507
9. Liu, Y., Liu, F., Iqbal, K., Grundke-Iqbal, I., & Gong, C. X. (2008). Decreased glucose transporters correlate to abnormal hyperphosphorylation of tau in Alzheimer disease. *FEBS letters*, *582*(2), 359–364. https://doi.org/10.1016/j.febslet.2007.12.035
10. An, Y., Varma, V. R., Varma, S., Casanova, R., Dammer, E., Pletnikova, O., Chia, C. W., Egan, J. M., Ferrucci, L., Troncoso, J., Levey, A. I., Lah, J., Seyfried, N. T.,

Legido-Quigley, C., O'Brien, R., & Thambisetty, M. (2018). Evidence for brain glucose dysregulation in Alzheimer's disease. *Alzheimer's & dementia : the journal of the Alzheimer's Association*, *14*(3), 318–329. https://doi.org/10.1016/j.jalz.2017.09.011

11. Swerdlow R. H. (2020). The mitochondrial hypothesis: Dysfunction, bioenergetic defects, and the metabolic link to Alzheimer's disease. *International review of neurobiology*, *154*, 207–233. https://doi.org/10.1016/bs.irn.2020.01.008
12. Bubber, P., Haroutunian, V., Fisch, G., Blass, J. P., & Gibson, G. E. (2005). Mitochondrial abnormalities in Alzheimer brain: mechanistic implications. *Annals of neurology*, *57*(5), 695–703. https://doi.org/10.1002/ana.20474
13. Parker, W. D., Jr, Parks, J., Filley, C. M., & Kleinschmidt-DeMasters, B. K. (1994). Electron transport chain defects in Alzheimer's disease brain. *Neurology*, *44*(6), 1090–1096. https://doi.org/10.1212/wnl.44.6.1090
14. Steen, E., Terry, B. M., Rivera, E. J., Cannon, J. L., Neely, T. R., Tavares, R., Xu, X. J., Wands, J. R., & de la Monte, S. M. (2005). Impaired insulin and insulin-like growth factor expression and signaling mechanisms in Alzheimer's disease--is this type 3 diabetes?. *Journal of Alzheimer's disease : JAD*, *7*(1), 63–80. https://doi.org/10.3233/jad-2005-7107
15. Arnold, S. E., Arvanitakis, Z., Macauley-Rambach, S. L., Koenig, A. M., Wang, H. Y., Ahima, R. S., Craft, S., Gandy, S., Buettner, C., Stoeckel, L. E., Holtzman, D. M., & Nathan, D. M. (2018). Brain insulin resistance in type 2 diabetes and Alzheimer disease: concepts and conundrums. *Nature reviews. Neurology*, *14*(3), 168–181. https://doi.org/10.1038/nrneurol.2017.185
16. Kumar, V., Kim, S. H., & Bishayee, K. (2022). Dysfunctional Glucose Metabolism in Alzheimer's Disease Onset and Potential Pharmacological Interventions. *International journal of molecular sciences*, *23*(17), 9540. https://doi.org/10.3390/ijms23179540
17. Leventhal, M. J., Zanella, C. A., Kang, B., Peng, J., Gritsch, D., Liao, Z., Bukhari, H., Wang, T., Pao, P. C., Danquah, S., Benetatos, J., Nehme, R., Farhi, S., Tsai, L. H., Dong, X., Scherzer, C. R., Feany, M. B., & Fraenkel, E. (2024). An integrative systems-biology approach defines mechanisms of Alzheimer's disease neurodegeneration. *bioRxiv : the preprint server for biology*, 2024.03.17.585262. https://doi.org/10.1101/2024.03.17.585262
18. Wang, M., Li, A., Sekiya, M., Beckmann, N. D., Quan, X., Schrode, N., Fernando, M. B., Yu, A., Zhu, L., Cao, J., Lyu, L., Horgusluoglu, E., Wang, Q., Guo, L., Wang, Y. S., Neff, R., Song, W. M., Wang, E., Shen, Q., Zhou, X., … Zhang, B.

(2021). Transformative Network Modeling of Multi-omics Data Reveals Detailed Circuits, Key Regulators, and Potential Therapeutics for Alzheimer's Disease. *Neuron*, *109*(2), 257–272.e14. https://doi.org/10.1016/j.neuron.2020.11.002

19. Beckmann, N. D., Lin, W. J., Wang, M., Cohain, A. T., Charney, A. W., Wang, P., Ma, W., Wang, Y. C., Jiang, C., Audrain, M., Comella, P. H., Fakira, A. K., Hariharan, S. P., Belbin, G. M., Girdhar, K., Levey, A. I., Seyfried, N. T., Dammer, E. B., Duong, D., Lah, J. J., … Schadt, E. E. (2020). Multiscale causal networks identify VGF as a key regulator of Alzheimer's disease. *Nature communications*, *11*(1), 3942. https://doi.org/10.1038/s41467-020-17405-z
20. Johnson ECB, Dammer EB, Duong DM, et al. Large-scale proteomic analysis of Alzheimer's disease brain and cerebrospinal fluid reveals early changes in energy metabolism associated with microglia and astrocyte activation. *Nat Med*. 2020;26(5):769-780. doi:10.1038/s41591-020-0815-6
21. Horgusluoglu, E., Neff, R., Song, W. M., Wang, M., Wang, Q., Arnold, M., Krumsiek, J., Galindo-Prieto, B., Ming, C., Nho, K., Kastenmüller, G., Han, X., Baillie, R., Zeng, Q., Andrews, S., Cheng, H., Hao, K., Goate, A., Bennett, D. A., Saykin, A. J., … Alzheimer Disease Metabolomics Consortium (2022). Integrative metabolomics-genomics approach reveals key metabolic pathways and regulators of Alzheimer's disease. *Alzheimer's & dementia : the journal of the Alzheimer's Association*, *18*(6), 1260–1278. https://doi.org/10.1002/alz.12468
22. Moon, S., & Lee, H. (2022). MOMA: a multi-task attention learning algorithm for multi-omics data interpretation and classification. *Bioinformatics (Oxford, England)*, *38*(8), 2287–2296. https://doi.org/10.1093/bioinformatics/btac080
23. Wang, J., Liao, N., Du, X., Chen, Q., & Wei, B. (2024). A semi-supervised approach for the integration of multi-omics data based on transformer multi-head self-attention mechanism and graph convolutional networks. *BMC genomics*, *25*(1), 86. https://doi.org/10.1186/s12864-024-09985-7
24. Egami, R., Kokaji, T., Hatano, A., Yugi, K., Eto, M., Morita, K., Ohno, S., Fujii, M., Hironaka, K. I., Uematsu, S., Terakawa, A., Bai, Y., Pan, Y., Tsuchiya, T., Ozaki, H., Inoue, H., Uda, S., Kubota, H., Suzuki, Y., Matsumoto, M., … Kuroda, S. (2021). Trans-omic analysis reveals obesity-associated dysregulation of inter-organ metabolic cycles between the liver and skeletal muscle. *iScience*, *24*(3), 102217. https://doi.org/10.1016/j.isci.2021.102217
25. Kokaji, T., Eto, M., Hatano, A., Yugi, K., Morita, K., Ohno, S., Fujii, M., Hironaka, K. I., Ito, Y., Egami, R., Uematsu, S., Terakawa, A., Pan, Y., Maehara, H., Li, D.,

Bai, Y., Tsuchiya, T., Ozaki, H., Inoue, H., Kubota, H., … Kuroda, S. (2022). In vivo transomic analyses of glucose-responsive metabolism in skeletal muscle reveal core differences between the healthy and obese states. *Scientific reports*, *12*(1), 13719. https://doi.org/10.1038/s41598-022-17964-9

26. Bai, Y., Morita, K., Kokaji, T., Hatano, A., Ohno, S., Egami, R., Pan, Y., Li, D., Yugi, K., Uematsu, S., Inoue, H., Inaba, Y., Suzuki, Y., Matsumoto, M., Takahashi, M., Izumi, Y., Bamba, T., Hirayama, A., Soga, T., & Kuroda, S. (2024). Trans-omic analysis reveals opposite metabolic dysregulation between feeding and fasting in liver associated with obesity. *iScience*, *27*(3), 109121. https://doi.org/10.1016/j.isci.2024.109121
27. Sugimoto, H., Morita, K., Li, D., Bai, Y., Mattanovich, M., & Kuroda, S. (2024). iTraNet: a web-based platform for integrated trans-omics network visualization and analysis. *Bioinformatics advances*, *4*(1), vbae141. https://doi.org/10.1093/bioadv/vbae141
28. Bennett DA, Schneider JA, Buchman AS, Barnes LL, Boyle PA, Wilson RS. Overview and findings from the rush Memory and Aging Project. *Curr Alzheimer Res*. 2012;9(6):646-663. doi:10.2174/156720512801322663
29. Bennett DA, Buchman AS, Boyle PA, Barnes LL, Wilson RS, Schneider JA. Religious Orders Study and Rush Memory and Aging Project. *J Alzheimers Dis*. 2018;64(s1):S161-S189. doi:10.3233/JAD-179939
30. Kanehisa M, Goto S. KEGG: kyoto encyclopedia of genes and genomes. *Nucleic Acids Res*. 2000;28(1):27-30. doi:10.1093/nar/28.1.27
31. Chang A, Jeske L, Ulbrich S, et al. BRENDA, the ELIXIR core data resource in 2021: new developments and updates. *Nucleic Acids Res*. 2021;49(D1):D498-D508. doi:10.1093/nar/gkaa1025
32. Wan YW, Al-Ouran R, Mangleburg CG, et al. Meta-Analysis of the Alzheimer's Disease Human Brain Transcriptome and Functional Dissection in Mouse Models. *Cell Rep*. 2020;32(2):107908. doi:10.1016/j.celrep.2020.107908
33. Wang, Q., Chen, K., Su, Y., Reiman, E. M., Dudley, J. T., & Readhead, B. (2021). Deep learning-based brain transcriptomic signatures associated with the neuropathological and clinical severity of Alzheimer's disease. *Brain communications*, *4*(1), fcab293. https://doi.org/10.1093/braincomms/fcab293
34. Wang, M., Beckmann, N. D., Roussos, P., Wang, E., Zhou, X., Wang, Q., Ming, C., Neff, R., Ma, W., Fullard, J. F., Hauberg, M. E., Bendl, J., Peters, M. A., Logsdon, B., Wang, P., Mahajan, M., Mangravite, L. M., Dammer, E. B., Duong, D. M., Lah, J. J., … Zhang, B. (2018). The Mount Sinai cohort of large-scale genomic,

transcriptomic and proteomic data in Alzheimer's disease. *Scientific data*, *5*, 180185. https://doi.org/10.1038/sdata.2018.185

35. De Jager, P. L., Ma, Y., McCabe, C., Xu, J., Vardarajan, B. N., Felsky, D., Klein, H. U., White, C. C., Peters, M. A., Lodgson, B., Nejad, P., Tang, A., Mangravite, L. M., Yu, L., Gaiteri, C., Mostafavi, S., Schneider, J. A., & Bennett, D. A. (2018). A multi-omic atlas of the human frontal cortex for aging and Alzheimer's disease research. *Scientific data*, *5*, 180142. https://doi.org/10.1038/sdata.2018.142
36. Zhou, Y., Zhou, B., Pache, L., Chang, M., Khodabakhshi, A. H., Tanaseichuk, O., Benner, C., & Chanda, S. K. (2019). Metascape provides a biologist-oriented resource for the analysis of systems-level datasets. *Nature communications*, *10*(1), 1523. https://doi.org/10.1038/s41467-019-09234-6
37. Johnson ECB, Carter EK, Dammer EB, et al. Large-scale deep multi-layer analysis of Alzheimer's disease brain reveals strong proteomic disease-related changes not observed at the RNA level. *Nat Neurosci*. 2022;25(2):213-225. doi:10.1038/s41593-021-00999-y
38. Batra, R., Arnold, M., Wörheide, M. A., Allen, M., Wang, X., Blach, C., Levey, A. I., Seyfried, N. T., Ertekin-Taner, N., Bennett, D. A., Kastenmüller, G., Kaddurah-Daouk, R. F., Krumsiek, J., & Alzheimer's Disease Metabolomics Consortium (ADMC) (2023). The landscape of metabolic brain alterations in Alzheimer's disease. *Alzheimer's & dementia : the journal of the Alzheimer's Association*, *19*(3), 980–998. https://doi.org/10.1002/alz.12714
39. Pang Z, Lu Y, Zhou G, et al. MetaboAnalyst 6.0: towards a unified platform for metabolomics data processing, analysis and interpretation. *Nucleic Acids Res*. 2024;52(W1):W398-W406. doi:10.1093/nar/gkae253
40. Reisberg, B., Doody, R., Stöffler, A., Schmitt, F., Ferris, S., Möbius, H. J., & Memantine Study Group (2003). Memantine in moderate-to-severe Alzheimer's disease. *The New England journal of medicine*, *348*(14), 1333–1341. https://doi.org/10.1056/NEJMoa013128
41. Martin FJ, Amode MR, Aneja A, et al. Ensembl 2023. *Nucleic Acids Res*. 2023;51(D1):D933-D941. doi:10.1093/nar/gkac958
42. Tasaki, S., Xu, J., Avey, D. R., Johnson, L., Petyuk, V. A., Dawe, R. J., Bennett, D. A., Wang, Y., & Gaiteri, C. (2022). Inferring protein expression changes from mRNA in Alzheimer's dementia using deep neural networks. *Nature communications*, *13*(1), 655. https://doi.org/10.1038/s41467-022-28280-1
43. Zou Z, Ohta T, Oki S. ChIP-Atlas 3.0: a data-mining suite to explore chromosome architecture together with large-scale regulome data. *Nucleic Acids Res*.

2024;52(W1):W45-W53. doi:10.1093/nar/gkae358
44. Zou Z, Ohta T, Miura F, Oki S. ChIP-Atlas 2021 update: a data-mining suite for exploring epigenomic landscapes by fully integrating ChIP-seq, ATAC-seq and Bisulfite-seq data. *Nucleic Acids Res*. 2022;50(W1):W175-W182. doi:10.1093/nar/gkac199
45. Koschützki, D., & Schreiber, F. (2008). Centrality analysis methods for biological networks and their application to gene regulatory networks. *Gene regulation and systems biology*, *2*, 193–201. https://doi.org/10.4137/grsb.s702
46. Koepsell H. Glucose transporters in brain in health and disease. *Pflugers Arch*. 2020;472(9):1299-1343. doi:10.1007/s00424-020-02441-x
47. Jankowska-Kulawy, A., Klimaszewska-Łata, J., Gul-Hinc, S., Ronowska, A., & Szutowicz, A. (2022). Metabolic and Cellular Compartments of Acetyl-CoA in the Healthy and Diseased Brain. *International journal of molecular sciences*, *23*(17), 10073. https://doi.org/10.3390/ijms231710073
48. Jia, D., Wang, F., & Yu, H. (2023). Systemic alterations of tricarboxylic acid cycle enzymes in Alzheimer's disease. *Frontiers in neuroscience*, *17*, 1206688. https://doi.org/10.3389/fnins.2023.1206688
49. Liang WS, Reiman EM, Valla J, et al. Alzheimer's disease is associated with reduced expression of energy metabolism genes in posterior cingulate neurons. *Proc Natl Acad Sci U S A*. 2008;105(11):4441-4446. doi:10.1073/pnas.0709259105
50. Jensen, N. J., Wodschow, H. Z., Nilsson, M., & Rungby, J. (2020). Effects of Ketone Bodies on Brain Metabolism and Function in Neurodegenerative Diseases. *International journal of molecular sciences*, *21*(22), 8767. https://doi.org/10.3390/ijms21228767
51. Hansmannel F, Sillaire A, Kamboh MI, et al. Is the urea cycle involved in Alzheimer's disease?. *J Alzheimers Dis*. 2010;21(3):1013-1021. doi:10.3233/JAD-2010-100630
52. Ju YH, Bhalla M, Hyeon SJ, et al. Astrocytic urea cycle detoxifies Aβ-derived ammonia while impairing memory in Alzheimer's disease. *Cell Metab*. 2022;34(8):1104-1120.e8. doi:10.1016/j.cmet.2022.05.011
53. Hernández-Ortega K, Garcia-Esparcia P, Gil L, Lucas JJ, Ferrer I. Altered Machinery of Protein Synthesis in Alzheimer's: From the Nucleolus to the Ribosome. *Brain Pathol*. 2016;26(5):593-605. doi:10.1111/bpa.12335
54. Szklarczyk D, Kirsch R, Koutrouli M, et al. The STRING database in 2023: protein-protein association networks and functional enrichment analyses for any

sequenced genome of interest. *Nucleic Acids Res*. 2023;51(D1):D638-D646. doi:10.1093/nar/gkac1000

55. Magistretti PJ, Allaman I. A cellular perspective on brain energy metabolism and functional imaging. *Neuron*. 2015;86(4):883-901. doi:10.1016/j.neuron.2015.03.035
56. Bonvento, G., & Bolaños, J. P. (2021). Astrocyte-neuron metabolic cooperation shapes brain activity. *Cell metabolism*, *33*(8), 1546–1564. https://doi.org/10.1016/j.cmet.2021.07.006
57. Shireby, G., Dempster, E. L., Policicchio, S., Smith, R. G., Pishva, E., Chioza, B., Davies, J. P., Burrage, J., Lunnon, K., Seiler Vellame, D., Love, S., Thomas, A., Brookes, K., Morgan, K., Francis, P., Hannon, E., & Mill, J. (2022). DNA methylation signatures of Alzheimer's disease neuropathology in the cortex are primarily driven by variation in non-neuronal cell-types. *Nature communications*, *13*(1), 5620. https://doi.org/10.1038/s41467-022-33394-7
58. Hannon, E., Dempster, E. L., Davies, J. P., Chioza, B., Blake, G. E. T., Burrage, J., Policicchio, S., Franklin, A., Walker, E. M., Bamford, R. A., Schalkwyk, L. C., & Mill, J. (2024). Quantifying the proportion of different cell types in the human cortex using DNA methylation profiles. *BMC biology*, *22*(1), 17. https://doi.org/10.1186/s12915-024-01827-y
59. Yu, L., Jin, J., Xu, Y., & Zhu, X. (2022). Aberrant Energy Metabolism in Alzheimer's Disease. *Journal of translational internal medicine*, *10*(3), 197–206. https://doi.org/10.2478/jtim-2022-0024
60. Nikkar, R., Esmaeili-Bandboni, A., Badrikoohi, M., & Babaei, P. (2022). Effects of inhibiting astrocytes and BET/BRD4 chromatin reader on spatial memory and synaptic proteins in rats with Alzheimer's disease. *Metabolic brain disease*, *37*(4), 1119–1131. https://doi.org/10.1007/s11011-022-00940-7
61. Matuszewska, M., Cieślik, M., Wilkaniec, A., Strawski, M., & Czapski, G. A. (2022). The Role of Bromodomain and Extraterminal (BET) Proteins in Controlling the Phagocytic Activity of Microglia In Vitro: Relevance to Alzheimer's Disease. *International journal of molecular sciences*, *24*(1), 13. https://doi.org/10.3390/ijms24010013
62. Sun, J., Gui, Y., Zhou, S., & Zheng, X. L. (2024). Unlocking the secrets of aging: Epigenetic reader BRD4 as the target to combatting aging-related diseases. *Journal of advanced research*, *63*, 207–218. https://doi.org/10.1016/j.jare.2023.11.006
63. Fu, W., Shi, D., Westaway, D., & Jhamandas, J. H. (2015). Bioenergetic mechanisms in astrocytes may contribute to amyloid plaque deposition and

toxicity. *The Journal of biological chemistry*, *290*(20), 12504–12513. https://doi.org/10.1074/jbc.M114.618157

64. Mathys, H., Boix, C. A., Akay, L. A., Xia, Z., Davila-Velderrain, J., Ng, A. P., Jiang, X., Abdelhady, G., Galani, K., Mantero, J., Band, N., James, B. T., Babu, S., Galiana-Melendez, F., Louderback, K., Prokopenko, D., Tanzi, R. E., Bennett, D. A., Tsai, L. H., & Kellis, M. (2024). Single-cell multiregion dissection of Alzheimer's disease. *Nature*, *632*(8026), 858–868. https://doi.org/10.1038/s41586-024-07606-7
65. McKinney, W. (2011). pandas: a foundational Python library for data analysis and statistics. *Python for high performance and scientific computing*, *14*(9), 1-9. https://doi.org/10.5281/zenodo.3509134
66. Hagberg, Aric, Swart, Pieter J., & Schult, Daniel A. (2008). Exploring network structure, dynamics, and function using NetworkX. https://doi.org/10.25080/TCWV9851
67. Hunter, J. D. (2007). Matplotlib: A 2D graphics environment. *Computing in science & engineering*, *9*(03), 90-95. https://doi.org/10.1109/MCSE.2007.55

1 **Supplementary text**

2 **Supplementary figures**

A

Item		Transcriptome		Proteome		Metabolome	
		AD	CT	AD	CT	AD	CT
Total subjects		156	87	71	74	144	61
Sex	male	46	39	14	28	35	26
	female	110	48	57	46	109	35
ApoE genotype	22	0	2	0	3	0	2
	23	9	14	4	15	10	11
	24	4	1	2	1	2	1
	33	82	62	49	50	75	42
	34	59	7	16	5	54	4
	44	2	1	0	0	3	1
Braak stage	0		5		3		4
	I		26		17		11
	II		14		14		13
	III		42		40		33
	IV	61		27		46	
	V	88		41		88	
	VI	7		3		10	
CERAD score	No AD		64		52		47
	Possible		23		22		14
	Probable	57		26		59	
	Definite	99		45		85	
Age at death	65~70	0	1	0	0	0	0
	70~75	1	7	0	2	0	2
	75~80	4	17	0	13	3	7
	80~85	15	19	4	17	12	11
	85~90	51	27	18	21	34	17
	Over 90	85	16	49	21	95	24
Postmortem interval (hours)	0~5	52	26	15	18	27	13
	5~10	74	45	43	42	94	39
	10~15	16	9	5	8	13	3
	15~20	11	6	4	2	7	3
	20~25	3	0	3	4	2	3
	25~30	0	1	0	0	0	0
	30~35	0	0	1	0	1	0

B

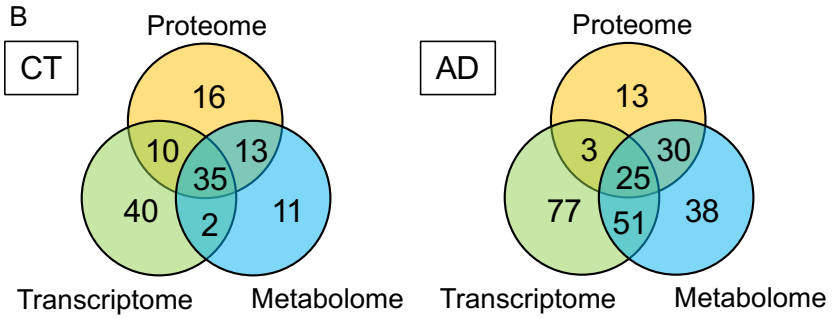

3

Figure S1. Information for the subjects from ROSMAP study.

(A) Information of the samples from ROSMAP Study used in this study, including sample size, sex, ApoE genotype, Braak Stage, CERAD score, age at death, and postmortem interval (PMI).

(B) Venn diagrams showing the overlap in data available for each subject across the three omic levels: transcriptome, proteome, and metabolome.

A

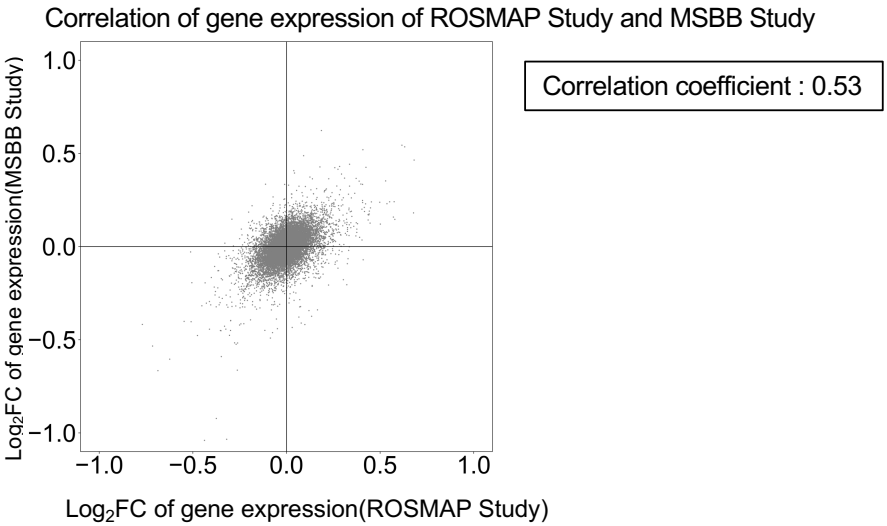

B

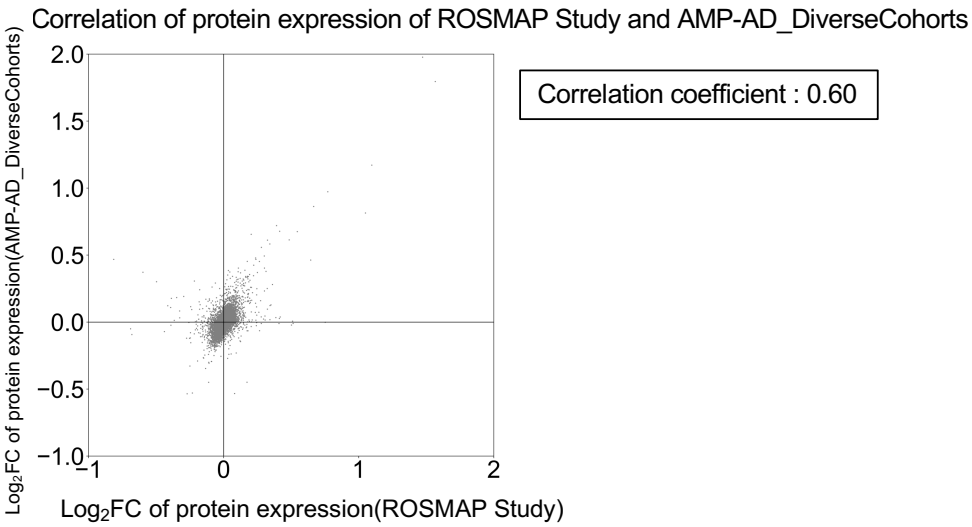

C

Reference	Increase	Decrease
Paglia, et al., 2016 (PMID: 26717242) • AD=21, CT=19 • Frontal cortex • UPLC-MS	acetylaspartic acid, pyruvate, glutamic acid, glutamine, SAMe, hydroxyproline, acetylglutamic acid, serine, SAM, threonine, choline, IMP	aspartic acid, xanthine, xanthosine, inosine
Xu, et al., 2016 (PMID: 26957286) • AD=9, CT=9 • Brain(hippocampus) • GC-MS	glucose, glucose-6-phosphate, sorbitol, fructose, pentonic acid B, arabinose, erythronic acid, lactic acid, 2-hydroxy-3-methylbutyric acid, threitol, xylitol, disaccharide, myo-inositol-1-phosphate, glycerol, glycerol-2-phosphate, glycerol-3-phosphate, citric acid, urea, creatinine, cysteine, tryptophan	ornithine, proline, lysine, serine, uracil, aspartic acid, ethanolamine, 2-hydroxyglutaric acid, ascorbic acid
Maffioli, et al., 2022 (PMID: 36070700) • AD=23, CT=20 • Hippocampal tissue • LC-MS and GC-MS	saccharopine, oxidized glutathione, mevalonate P, arginine, guanidoacetic acid, D-glucose, deoxyuridine, beta-D-gluocse-6-phosphate, AICAR, urea, succinic acid, erythrose-4-phosphate, glycerol-3-phosphate	uridine 5' diphosphate, pyruvic acid, O Acetyl ADP ribose, mevalonate PP, L-Lysine, L-lactic acid, glutathione, glucosamine 6 phosphate, citrulline, L-alanine, uracil

Figure S2. Comparison of transcriptome, proteome, and metabolome data from the ROSMAP Study with data from other studies.

(A) Correlation between two transcriptomic datasets obtained from the ROSMAP Study and the MSSB Study for each gene. In the MSSB Study, RNA sequencing data were collected from brain tissue (FP; frontal pole) of individuals with AD (45 AD patients) and control subjects (45 CT subjects). For correlation analysis, the $\log_2$ fold-change values in 16,348 genes were calculated by dividing the average expression of the AD group by the average expression of the CT group.

(B) Correlation between two proteomic datasets obtained from the ROSMAP Study and AMP-AD_DiverseCohorts for each protein. TMT-MS data from each study were from brain tissue (DLPFC) of individuals with AD (637 AD patients) and control subjects (224 CT subjects). Correlation analysis was performed on the $\log_2$ fold-change values (average abundance of AD divided by average abundance of CT) for 9,180 proteins.

(C) Differentially expressed metabolites (DEMs) identified in previous studies [1,2,3]. Note that each study used different definitions for AD and CT groups, had variations in measurement methods and brain regions analyzed. These studies had smaller sample sizes than our study.

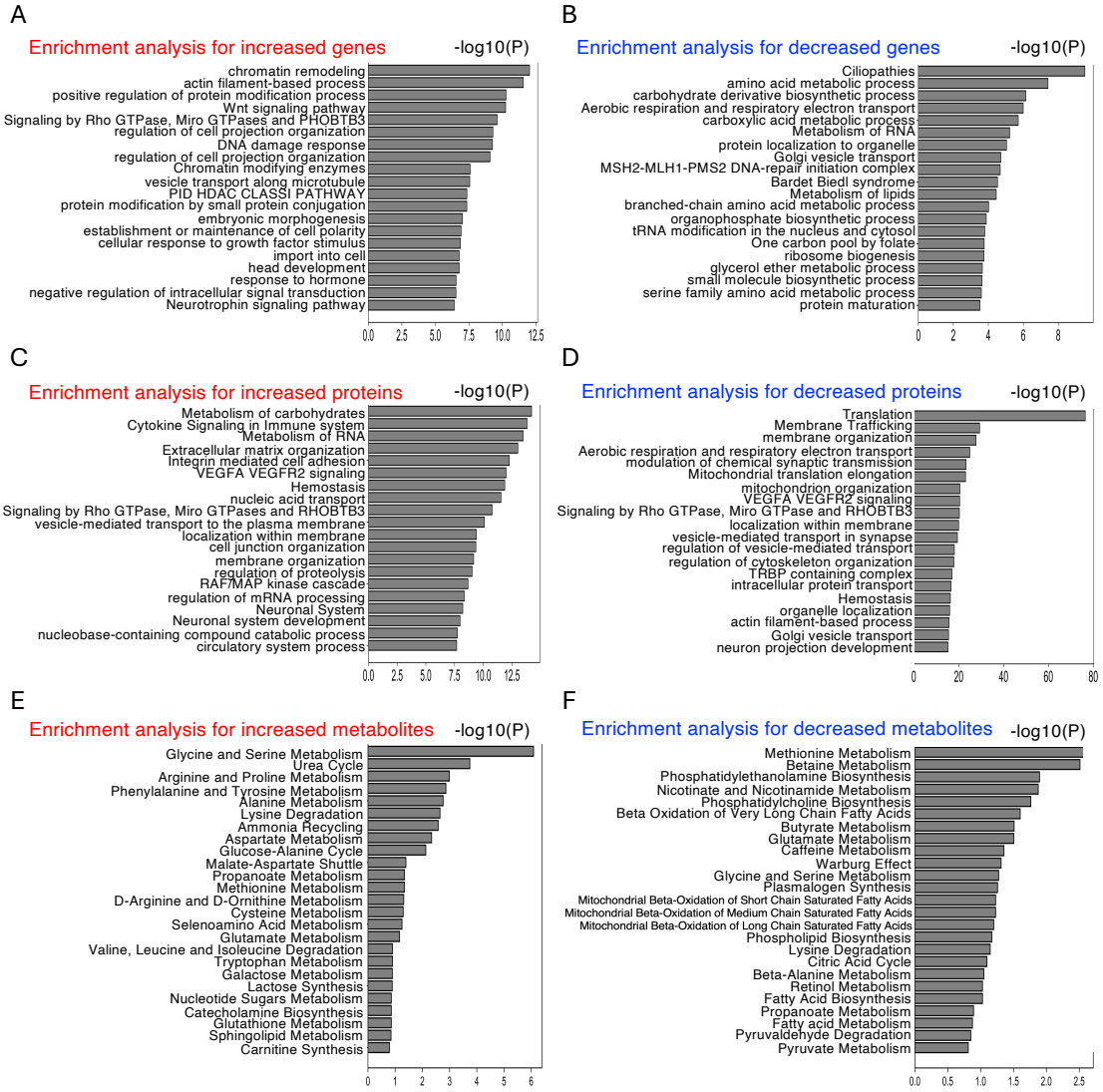

Figure S3. Enrichment analysis for differentially expressed molecules of AD.

(A) Enrichment analysis for increased DEGs in AD performed with Metascape.

(B) Enrichment analysis for decreased DEGs in AD performed with Metascape.

(C) Enrichment analysis for increased DEPs in AD performed with Metascape.

(D) Enrichment analysis for decreased DEPs in AD performed with Metascape.

(E) Enrichment analysis for increased DEMs in AD performed with MetaboAnalyst.

(F) Enrichment analysis for decreased DEMs in AD performed with MetaboAnalyst.

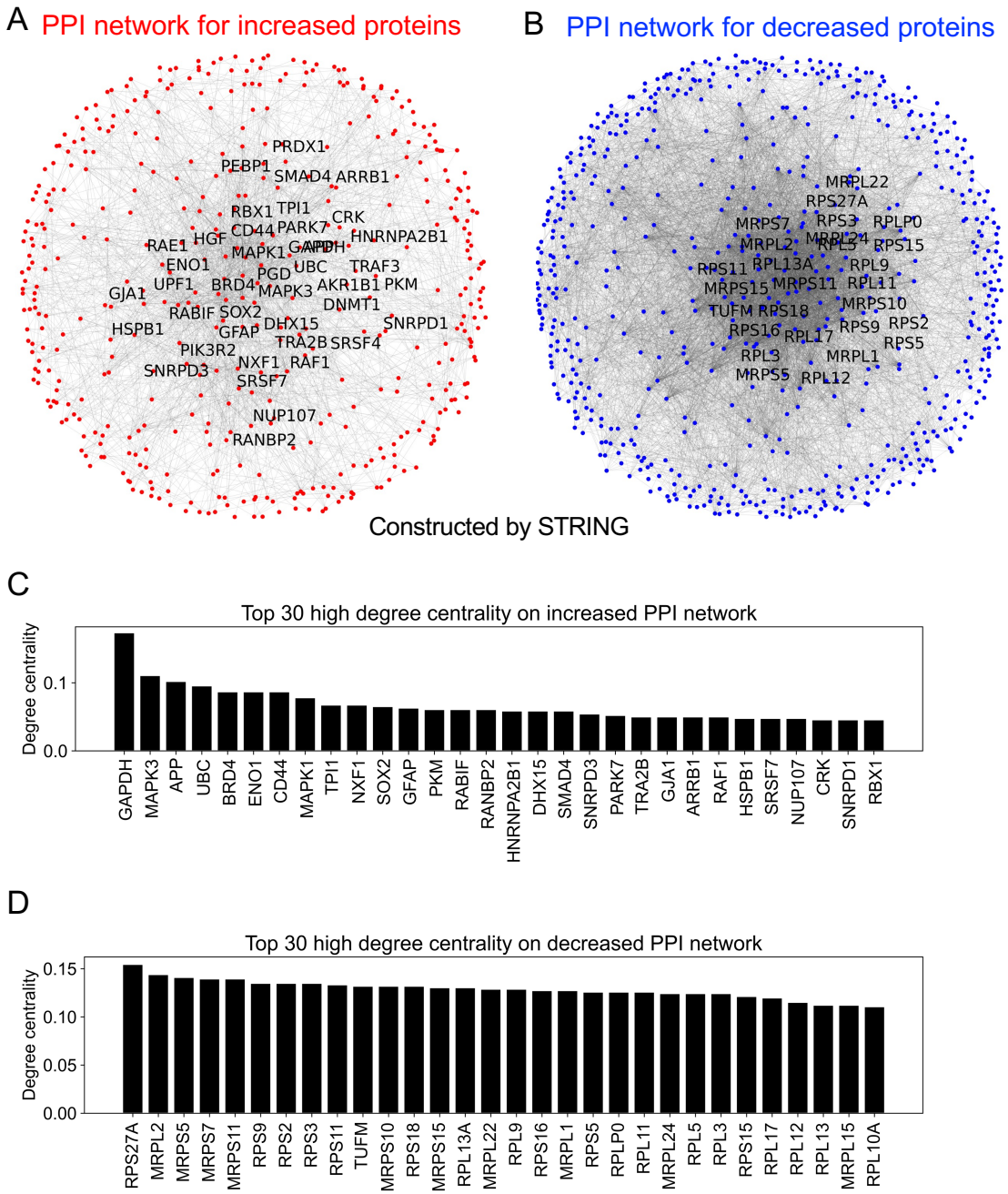

Figure S4. Construction of protein-protein interaction networks in DLPFC of AD.

(A) The protein-protein interaction (PPI) network for increased DEPs. Red nodes and gray edges indicated DEPs and their interactions, respectively. The nodes whose degree are over 18 their degree centralities are labeled for reasons of legibility (Supplementary Data 2).

(B) The PPI network for decreased DEPs. Blue nodes and gray edges indicated DEPs and their interactions, respectively. The nodes whose degree are over 75 their degree centralities are labeled for reasons of legibility (Supplementary Data 2).

(C) Top 30 DEPs with high degree centrality on the increased PPI network.

(D) Top 30 DEPs with high degree centrality on the decreased PPI network.

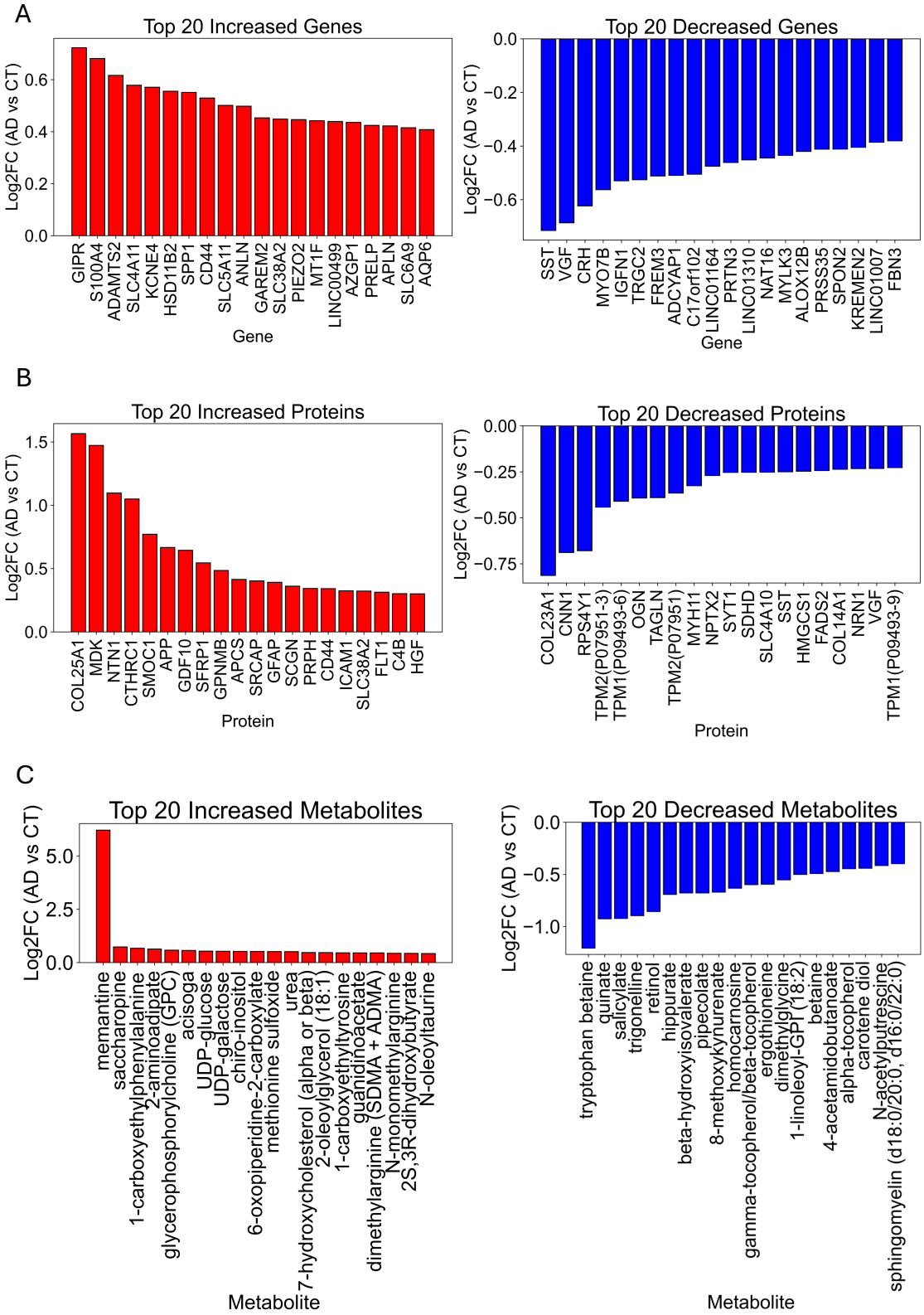

Figure S5. Top 20 differentially expressed genes, proteins, and metabolites.
(A) The top 20 differentially expressed genes (DEGs) ranked and plotted according to

log_2 fold change (Log2FC) in mean expression between AD and CT. Red, DEGs with increased expression in AD (left); blue, DEGs with decreased expression in AD (right).

(B) The top 20 differentially expressed proteins (DEPs) ranked and plotted according to log_2 fold change (Log2FC) in mean expression between AD and CT. Red, DEPs with increased expression in AD (left); blue, DEPs with decreased expression in AD (right).

(C) The top 20 differentially expressed metabolites (DEMs) ranked and plotted according to log_2 fold change (Log2FC) in mean expression between AD and CT. Red, DEMs with increased expression in AD (left); blue, DEMs with decreased expression in AD (right).

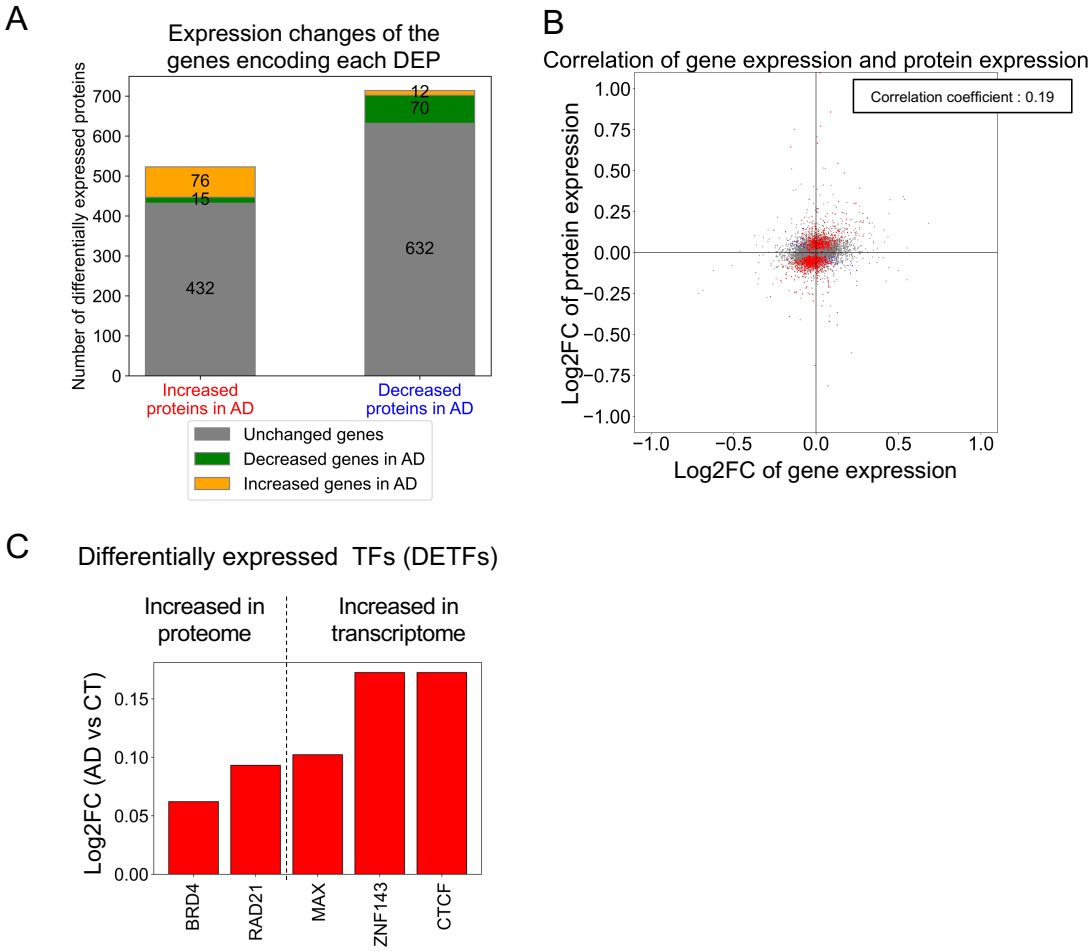

Figure S6. Identification of differential regulations connecting differentially expressed molecules across different omic layers.

(A) The change in the encoding gene for the corresponding DEP grouped according to the increased DEPs and decreased DEPs in AD.

(B) Correlation of the $\log_2$ fold changes (AD group vs. CT group) of measured molecules at the transcriptome level (x-axis) and proteome level (y-axis). Each point on a scatter plot represents a molecule measured as both mRNA and protein. DEPs are shown in blue or red. Blue represents those DEPs with encoding DEGs that change in the opposite direction; Red represents the rest of the DEPs.

(C) Log_2 fold change (AD group vs. CT group) of each differentially expressed transcription factor (DETF). The log2 fold change (Log2FC) of gene expression (transcriptome) or protein expression (proteome) of the indicated DETFs, which were identified from the 19 TFs that were inferred as potential regulators of DEGs with significantly altered expression in AD.

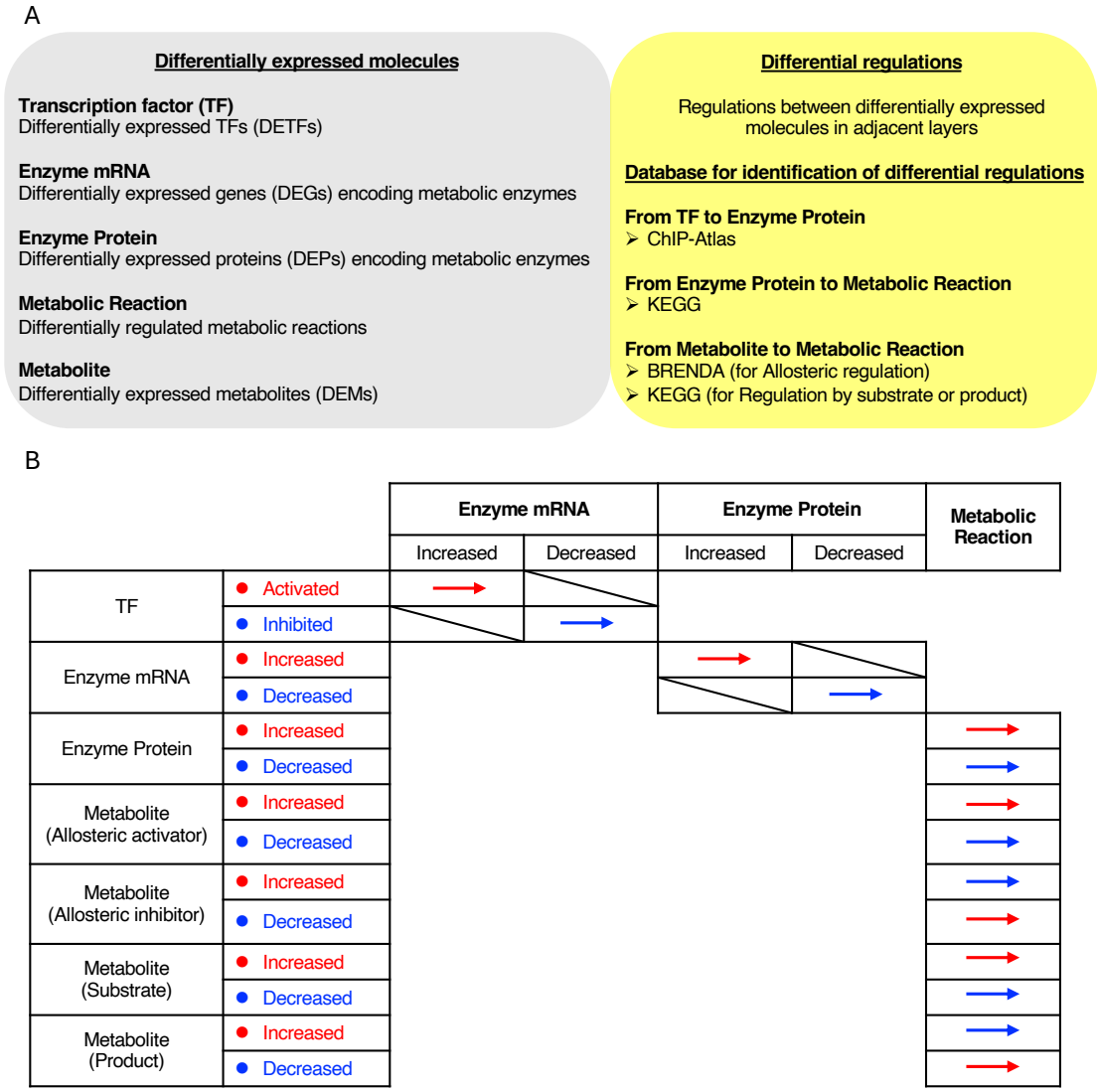

Figure S7. Contents of the trans-omic network for differentially regulated metabolic reactions between CT and AD.

(E) The definition of differentially expressed molecules in each layer (left). Differential regulations between adjacent layers and the databases used to identify them (right).

(F) Classification of the differential regulations (activating or inhibiting in AD group) based on the altered direction of differentially expressed molecules and the characteristics of the metabolite (allosteric activator, allosteric inhibitor, substrate, or product). The methodology of constructing differential regulatory trans-omic network of metabolic reactions is based on our previous study [4,5].

Supplementary text

Validation of the results of enrichment analysis. Related to Fig. S3.

Enrichment analysis using Metascape revealed that genes with significantly increased expression were primarily enriched in functions related to the cytoskeleton and signal transduction, whereas genes with significantly decreased expression were enriched in functions related to mitochondria and RNA metabolism (Fig. S3A and S3B). Our results of the enrichment analysis for transcriptome are consistent with the previous studies. One study identified genes related to stress response, cell-matrix adhesion, MAPKKK cascade, and cell proliferation as upregulated in the CA1 region of AD patients, and genes associated with synaptic transmission, cell-cell signaling, and neurogenesis as downregulated [9]. Another study focusing on gene expression in the hippocampus of AD patients reported significant changes in gene expression related to metal ion transport, synaptic transmission, mitochondria, and RNA processing [10]. Enrichment analysis performed on samples obtained from the middle temporal gyrus indicated changes in gene expression related to the synaptic vesicle cycle, GABAergic synapse, insulin secretion, gap junction, and synaptic vesicle transport [11].

Enrichment analysis using Metascape showed that proteins with significantly increased expression were enriched in functions related to metabolism of carbohydrates and membrane processes; proteins with significantly decreased expression were enriched in functions related to the cytoskeleton, vesicle transport, translation, and mitochondrial functions (Fig. S3C and S3D). A meta-analysis study on the proteome of AD reported that proteins related to synaptic signaling, vesicle-mediated transport in synapses, and mitochondrial ATP synthesis electron transport were enriched in proteins with significantly decreased expression. In contrast, wound response and inflammatory response were enriched in proteins with significantly increased expression [12]. Our results agree with these results.

Enrichment analysis using MetaboAnalyst identified metabolites with significantly increased expression as enriched in various amino acid metabolism pathways, as well as nitrogen metabolism pathways such as the urea cycle and ammonia recycling (Fig. S3E). Metabolites with significantly decreased expression were enriched in pathways related to methionine and betaine metabolism (Fig. S3F). A previous study that quantified ATP in mouse model of AD reported that ATP levels significantly decrease with age in these mice [13]. A previous study that measured the metabolome of the frontal cortex of AD patients and CT subjects showed significant increases in pyruvate,

glutamate, glutamine, serine, and threonine, consistent with our findings [1]. In the same study, pathway analysis indicated that alanine, aspartate, and glutamate metabolism, arginine and proline metabolism, cysteine and methionine metabolism, and glycine, serine, and threonine metabolism are affected by AD progression [1], which is consistent with our findings.

Top 20 differentially expressed genes, proteins, metabolites. (Fig. S5)

We identified the top 20 increased and top 20 decreased DEGs based on their $\log_2$ fold change (log2FC) values (AD group vs. CT group) for their mean values (Fig. S5A). *GIPR*, which has been reported to have neuroprotective effects [6], and the inflammation-associated gene *CD44* were identified as DEGs with high log2FC values. *SST*, encoding the neuropeptide somatostatin, was identified among the DEGs with the lowest log2FC values.

We also identified the top 20 upregulated and top 20 downregulated DEPs based on their $\log_2$ fold change (log2FC) values (Fig. S5B). DEPs with high log2FC values included SIRPB1, which promotes phagocytosis by microglia [7], and GFAP, a candidate blood biomarker of AD [8]. DEPs with low log2FC values included those associated with the cytoskeleton, such as CNN1, TMP1, and TMP2.

We also identified the top 20 DEMs with the highest and lowest log2 fold change (log2FC) values (Fig. S5C). Notably, memantine was identified as the metabolite with the highest log2FC value. Memantine is a therapeutic drug for Alzheimer's disease. Therefore, it does not seem to be related to the pathology of the disease itself. However, this means that our analysis can accurately detect the differences between CT and AD groups. Retinol and sphingomyelin showed the lowest log2FC values.

Protein-protein interaction networks for the DEPs in AD. (Fig. S4)

The multi-omic data used in this study contains not only metabolism, but also more general cellular mechanisms such as gene-regulatory network and protein-protein interactions. Therefore, we constructed protein-protein interaction (PPI) networks using DEPs with STRING [14] (Fig. S4A, S4B and Supplementary Data 2). We then examined the degree centralities of the nodes on the PPI networks (Fig. S4C, S4D). In the "Increased PPI" network, GAPDH emerged as the protein with the highest degree centrality. GAPDH is not only an enzyme in the glycolytic pathway but also plays roles in apoptosis, neurodegeneration, cognitive dysfunction, and the formation of aggregates

with Aβ [15]. In contrast, in the “Decreased PPI” network, nearly all the top 30 proteins by degree centrality were ribosomal proteins or mitochondrial ribosomal proteins. These results suggested that AD is associated with reduced translation both in nucleus and mitochondria.

1 **Supplementary tables**

2 **Table S1. A list of transcription factors inferred to be involved in the regulation of**

3 **DEGs in DLPFC of AD.**

Classification	TF Name
for Increased Gene	CTCF, MAX, MYCN, OLIG2, KDM1A, CTCFL, ARID1A, LIN28B, GTF3C2, CHD8, SMC3, ZNF92, TOP2B, ZNF143, EP300, TEAD4, BRD4, RAD21, BRD2
for Decreased Gene	None

4

5

1 **Table S2. A list of differentially expressed metabolic enzymes in DLPFC of AD.**

Increased enzymes	ACAT2, AK1, AKR1B1, ALDH3A2, AMPD2, ASL, B4GALNT1, BBOX1, BLVRA, BLVRB, CA3, CAD, CBR3, CBS, CMBL, DGKG, DNMT1, ENO1, ESD, FAH, GALK1, GALM, GALNT16, GAPDH, GBE1, GMPR, GSTP1, INPP4B, ITPKB, LPIN1, LTA4H, MAN2A2, MAOB, MTAP, MTHFD1, MTHFD2L, NAGK, NT5C, NUDT16, OCRL, PAFAH1B3, PGAM2, PGD, PGLS, PHYKPL, PI4K2A, PKM, PLCD1, PLCD3, PPT1, PRDX6, QPRT, RBKS, RENBP, SAT2, SORD, TPI1, UGP2, UROD
Decreased enzymes	ABHD16A, ACAA2, ACOX1, ACSS1, ADCY1, ADCY2, AGPAT1, AGPAT3, AHCYL1, ALDH4A1, ALPL, AOC3, BCAT2, BCKDHB, BDH1, BPNT2, CDIPT, CS, CTH, DBT, DGKH, DGKI, DGKZ, DLD, ECHS1, FADS2, FDFT1, GAD1, GAD2, GGT5, GK, GLDC, GPHN, GSTK1, HMGCL, HMGCS1, HMOX2, HSD17B12, IDH2, L2HGDH, LCLAT1, MBOAT2, MECR, MGLL, MGST3, MT-ND3, MTMR7, NAT8L, NDUFS1, NDUFS7, NDUFS8, NDUFV1, NFS1, NNT, NOS1, NT5E, PDE4A, PDE4B, PGM2L1, PIP5K1A, PIP5K1C, PLCB1, PRPS2, PYCR2, RRM1, SDHA, SETD7, SHMT2, SMPD3, TM7SF2

2

Supplementary data

Supplementary_Data_1.xlsx: Trans-Omic network for metabolic reactions in AD

Supplementary_Data_2.xlsx: Protein-protein interaction networks in AD

Supplementary references

1. Paglia G, Stocchero M, Cacciatore S, et al. Unbiased Metabolomic Investigation of Alzheimer's Disease Brain Points to Dysregulation of Mitochondrial Aspartate Metabolism. *J Proteome Res*. 2016;15(2):608-618. doi:10.1021/acs.jproteome.5b01020
2. Xu J, Begley P, Church SJ, et al. Graded perturbations of metabolism in multiple regions of human brain in Alzheimer's disease: Snapshot of a pervasive metabolic disorder. *Biochim Biophys Acta*. 2016;1862(6):1084-1092. doi:10.1016/j.bbadis.2016.03.001
3. Maffioli E, Murtas G, Rabattoni V, et al. Insulin and serine metabolism as sex-specific hallmarks of Alzheimer's disease in the human hippocampus. *Cell Rep*. 2022;40(10):111271. doi:10.1016/j.celrep.2022.111271
4. Bai, Y., Morita, K., Kokaji, T., Hatano, A., Ohno, S., Egami, R., Pan, Y., Li, D., Yugi, K., Uematsu, S., Inoue, H., Inaba, Y., Suzuki, Y., Matsumoto, M., Takahashi, M., Izumi, Y., Bamba, T., Hirayama, A., Soga, T., & Kuroda, S. (2024). Trans-omic analysis reveals opposite metabolic dysregulation between feeding and fasting in liver associated with obesity. *iScience*, *27*(3), 109121. https://doi.org/10.1016/j.isci.2024.109121
5. Egami, R., Kokaji, T., Hatano, A., Yugi, K., Eto, M., Morita, K., Ohno, S., Fujii, M., Hironaka, K. I., Uematsu, S., Terakawa, A., Bai, Y., Pan, Y., Tsuchiya, T., Ozaki, H., Inoue, H., Uda, S., Kubota, H., Suzuki, Y., Matsumoto, M., … Kuroda, S. (2021). Trans-omic analysis reveals obesity-associated dysregulation of inter-organ metabolic cycles between the liver and skeletal muscle. *iScience*, *24*(3), 102217. https://doi.org/10.1016/j.isci.2021.102217
6. Reich, N., & Hölscher, C. (2022). The neuroprotective effects of glucagon-like peptide 1 in Alzheimer's and Parkinson's disease: An in-depth review. *Frontiers in neuroscience*, *16*, 970925. https://doi.org/10.3389/fnins.2022.970925
7. Gaikwad S, Larionov S, Wang Y, et al. Signal regulatory protein-beta1: a microglial modulator of phagocytosis in Alzheimer's disease. *Am J Pathol*. 2009;175(6):2528-2539. doi:10.2353/ajpath.2009.090147
8. Kim, K. Y., Shin, K. Y., & Chang, K. A. (2023). GFAP as a Potential Biomarker for Alzheimer's Disease: A Systematic Review and Meta-Analysis. *Cells*, *12*(9), 1309. https://doi.org/10.3390/cells12091309
9. Miller, J. A., Woltjer, R. L., Goodenbour, J. M., Horvath, S., & Geschwind, D. H. (2013). Genes and pathways underlying regional and cell type changes in

Alzheimer's disease. *Genome medicine*, *5*(5), 48. https://doi.org/10.1186/gm452

10. Miller JA, Oldham MC, Geschwind DH. A systems level analysis of transcriptional changes in Alzheimer's disease and normal aging. *J Neurosci*. 2008;28(6):1410-1420. doi:10.1523/JNEUROSCI.4098-07.2008
11. Piras IS, Krate J, Delvaux E, et al. Transcriptome Changes in the Alzheimer's Disease Middle Temporal Gyrus: Importance of RNA Metabolism and Mitochondria-Associated Membrane Genes. *J Alzheimers Dis*. 2019;70(3):691-713. doi:10.3233/JAD-181113
12. Askenazi, M., Kavanagh, T., Pires, G., Ueberheide, B., Wisniewski, T., & Drummond, E. (2023). Compilation of reported protein changes in the brain in Alzheimer's disease. *Nature communications*, *14*(1), 4466. https://doi.org/10.1038/s41467-023-40208-x
13. Zhang C, Rissman RA, Feng J. Characterization of ATP alternations in an Alzheimer's disease transgenic mouse model. *J Alzheimers Dis*. 2015;44(2):375-378. doi:10.3233/JAD-141890
14. Szklarczyk D, Kirsch R, Koutrouli M, et al. The STRING database in 2023: protein-protein association networks and functional enrichment analyses for any sequenced genome of interest. *Nucleic Acids Res*. 2023;51(D1):D638-D646. doi:10.1093/nar/gkac1000
15. Lazarev, V. F., Tsolaki, M., Mikhaylova, E. R., Benken, K. A., Shevtsov, M. A., Nikotina, A. D., Lechpammer, M., Mitkevich, V. A., Makarov, A. A., Moskalev, A. A., Kozin, S. A., Margulis, B. A., Guzhova, I. V., & Nudler, E. (2021). Extracellular GAPDH Promotes Alzheimer Disease Progression by Enhancing Amyloid-β Aggregation and Cytotoxicity. *Aging and disease*, *12*(5), 1223–1237. https://doi.org/10.14336/AD.2020.1230